C.P. No. 975

C.P. No. 975

MINISTRY OF TECHNOLOGY

AERONAUTICAL RESEARCH COUNCIL

CURRENT PAPERS

Optimum Fibre Arrangements for Reinforced Sheets Under Combined Loading

by

G. Z. Harris, Ph.D.

LONDON. HER MAJESTY'S STATIONERY OFFICE

1968

PRICE 13s 6d NET

U.D.C. No.621-419.9 : 620.172.2 : 539.42 : 539.376

C.P. No.975*
November 1966

OPTIMUM FIBRE ARRANGEMENTS FOR REINFORCED SHEETS UNDER COMBINED LOADING

by

G. Z. Harris, Ph.D.

SUMMARY

Sheets having three directions of fibre reinforcement are considered on the basis of netting analysis. Load envelopes of shear combined with both uniaxial and biaxial tension are assumed and optimum fibre arrangements are determined on the assumption that limits exist on the compressive and tensile forces which may be developed in a fibre. Such optimum fibre arrangements are compared with the best-arranged isotropic reinforced sheets and with hypothetical solid sheets having the same properties as the fibres. The total allowable load envelopes of the optimum arrangements are derived and are related to the prescribed load envelopes. The elastic constants of the optimum systems are also derived.

---

* Replaces R.A.E. Technical Report 66361 - A.R.C. 29320

CONTENTS

1 INTRODUCTION

Numerous materials exist having high tensile strengths and high elastic moduli which, in the large, are imperfection-sensitive. Such materials may, however, be produced in imperfection-free form as fibres which allow high tensile strength and stiffness to be achieved, albeit in a limited form. Particularly when combined with low density this provides a considerable attraction and has led to the production of composite materials in which fibres are used to reinforce a matrix material. The form in which the reinforcement is incorporated in the matrix may vary; fibres may be orientated either randomly or in a regular manner, and at different volume fractions, depending on the properties which are required in the composite. Paper, for example, is basically a sheet of fibres randomly orientated in a plane and packed at high volume fraction; the elastic behaviour of such materials has been studied for some time (see, for example, Cox[1]). Glass-fibre filaments are also used in the construction of pressure vessels and studies have been made to determine optimum properties[2,3] in such cases. Glass-fibre is also used in the construction of directionally reinforced laminated and sandwich materials. All these applications generally aim at achieving high fibre volume-fractions to reproduce as far as possible the desirable properties of the fibre in material form.

The properties of composite materials depend in general on the material properties of both the fibres and the matrix and analysis which takes this into account is essential when considering, for example, the properties of unidirectionally reinforced composites[4] in directions inclined to the fibres. However, in a large class of problems[1,2,3] a consistent physical model is possible in which the applied load system can be entirely carried as axial load in the fibres without any assistance from the matrix insofar as load-carrying capacity is concerned. Analysis based on this assumption is usually referred to as 'netting' analysis since the mechanism for carrying load is that of a fibre-network. Now a sheet with unidirectional reinforcement can be regarded as carrying loads having that direction entirely in the fibres, its resistance to loads in other directions depending to a considerable degree on the properties of the matrix. A cross-ply sheet reinforced in two orthogonal fibre-directions will carry in the fibres loads which are applied in these directions; resistance to shear, however, will again depend to a large degree on the shear properties of the matrix. The simplest directionally reinforced sheet able to carry general applied loading systems

as forces in the fibres is thus one which is reinforced in three different directions and it is composites of this type which are considered on the basis of netting analysis in this Report. The material properties of a reinforced sheet containing continuous fibres aligned in three directions will depend to a considerable degree on the angles of alignment and the numbers of fibres in any direction. For example, an arrangement having equal numbers of fibres the angles between whose directions are 60° and 120° is one possible arrangement and behaves elastically as an isotropic sheet having a Poisson's ratio of 1/3. This Paper considers sheets having fibres aligned in three directions where the quantities and directions of the fibres are optimised with regard to some assigned load envelope. A three-directional network is statically determinate and no appeal to the elastic properties of the fibres is necessary.

General expressions are derived in Section 2 for the load carried in any fibre direction when a load system is applied. The optimum fibre quantities and directions can then be found and this is done in Sections 3-5 for sheets which are subjected to uniform uniaxial and biaxial tensions together with a shear. Uniaxial tension combined with shear is typical, for example, of a wing or fuselage under-panel which derives tension from bending and shear from torsion. Biaxial tension combined with shear is typical of a pressure cabin panel, the biaxial tensions arising from pressurisation and the shear from fuselage torsion. Since isotropic sheet is a standard form in which reinforced materials are made-up, a comparison is made between the densities of optimum sheet and the optimum isotropic reinforced sheet required to carry the same load system. A sheet subjected to uniaxial tension aligned in any arbitrary direction is also considered in Section 6. The use of netting analysis is particularly welcome since the optimisations carried out here would be difficult under a theory which accounted also for the properties of the matrix. Further, since matrix-fibre combinations differ in their properties it is relevant to perform an analysis in which only the fibre properties are considered. In practical cases it is important to know the total load envelopes which can be carried by the systems, and these are considered in Section 7 for the systems of reinforcement which arise. Although the optimisations carried out make no use of fibre elasticity, the elastic constants of optimum systems are clearly of interest and these are derived in Appendix A.

There is a similarity between the optimisation of a statically determinate fibre net with respect to a given load envelope and the optimisation of a plane framework with respect to a finite number of distinct loading conditions. The theory of Michell structures, which deals with the problem of determining the minimum-weight framework able to carry a single load system applied at specified points in space, has been summarised by Cox[5]. Extensions of this theory to allow consideration of a number of loading conditions have been indicated by Schmidt[6]. However in the field of Michell structures, frames consisting of numbers of members are derived to accommodate loads applied at distinct points in space whereas the present Paper is concerned with the optimisation of three fibre directions for a continuous envelope of load.

Now fibre reinforcement must appear inefficient if considered solely as a mode of construction for a material available in other forms. A solid sheet of any conventional material is capable of carrying a combined load-system of tension and shear which is determined by a yield criterion such as the Mises-Hencky (see, for example, Hill[7]). The same material prepared in a fibre form and made-up into a unidirectional composite would be able to carry the same unidirectional tensile load as the solid material, but its capacity to carry other loads would be severely impaired. In addition, the composite would be heavier since a matrix material would have been added. The argument in favour of composite materials is that, although they must seem inefficient if their form of construction alone is considered, the fibres are not available in other forms and their properties are so attractive that this inefficiency can be more than offset. Thus, to make a valid assessment of the efficiency of composites on the basis of comparing like with like, comparisons are also made in this Report between the densities of reinforced and 'solid' sheets optimised to carry the same load system; in view of the above remarks the existence of such solid sheet is hypothetical but the comparison is necessary to enable the further comparison between reinforced and conventional materials to be made meaningfully.

2 GENERAL EQUATIONS

Consider a rectangular sheet having sides parallel to the co-ordinate axes $O(x,y)$ in which continuous fibres are arranged in parallel systems having three directions α, β and γ, defined so that

$$180^\circ \geq \gamma > \beta > \alpha > 0$$

(see Fig.1). Although individual fibres may vary in cross-sectional area, strength etc., an assemblage of average fibres with average properties will be assumed; the disposition of these fibres in the plane of the panel is such that they are arranged at densities of p, q and r fibres per unit distance, while the corresponding tensile forces in single fibres are P, Q and R. The sheet is subjected to an applied load-system,

$$(N_x, N_y, N_{xy}) = (T_1, T_2, S) \qquad (1)$$

as shown in Fig.1; N_x etc. and T_1 etc. have the dimensions of force per unit length. Equations for P, Q, R are derived by considering equilibrium of the sheet. Equilibrium at the sides x = constant gives

$$\left.\begin{aligned} p\,P\cos^2\alpha + q\,Q\cos^2\beta + r\,R\cos^2\gamma &= T_1, \\ p\,P\sin\alpha\cos\alpha + q\,Q\sin\beta\cos\beta + r\,R\sin\gamma\cos\gamma &= S, \end{aligned}\right\}$$

while equilibrium at the sides y = constant gives

$$\left.\begin{aligned} p\,P\sin\alpha\cos\alpha + q\,Q\sin\beta\cos\beta + r\,R\sin\gamma\cos\gamma &= S, \\ p\,P\sin^2\alpha + q\,Q\sin^2\beta + r\,R\sin^2\gamma &= T_2. \end{aligned}\right\}$$

Since the equation related to equilibrium of shear is the same in each case, these equations reduce to

$$\left.\begin{aligned} p\,P + q\,Q + r\,R &= T_1 + T_2, \\ p\,P\cos 2\alpha + q\,Q\cos 2\beta + r\,R\cos 2\gamma &= T_1 - T_2, \\ p\,P\sin 2\alpha + q\,Q\sin 2\beta + r\,R\sin 2\gamma &= 2S, \end{aligned}\right\} \qquad (2)$$

which determine P, Q and R completely. The solution of equation (2) is

$$\left.\begin{aligned} p\,P\,\sin(\beta-\alpha)\,\sin(\gamma-\alpha) &= T_1 \sin\beta \sin\gamma + T_2 \cos\beta\cos\gamma - S\sin(\beta+\gamma), \\ q\,Q\,\sin(\alpha-\beta)\,\sin(\gamma-\beta) &= T_1 \sin\gamma \sin\alpha + T_2 \cos\gamma\cos\alpha - S\sin(\gamma+\alpha), \\ r\,R\,\sin(\beta-\gamma)\,\sin(\alpha-\gamma) &= T_1 \sin\alpha \sin\beta + T_2 \cos\alpha\cos\beta - S\sin(\alpha+\beta). \end{aligned}\right\} \quad (3)$$

Equation (3) is general. If systems of reinforcement symmetric with respect to Ox are considered, then either

$$\beta = 180^\circ - \alpha, \qquad \gamma = 180^\circ, \qquad p = q, \qquad (4)$$

which will be referred to in what follows as longitudinally symmetric (abbreviated to l.s.) systems, or

$$\beta = 90^\circ, \qquad \gamma = 180^\circ - \alpha, \quad p = r, \qquad (5)$$

which will be referred to as transversely symmetric (t.s.) systems.
The l.s. system of equation (4) then gives for the forces in the fibres

$$\left.\begin{aligned} p\,P &= \tfrac{1}{2} T_2 \operatorname{cosec}^2\alpha + S \operatorname{cosec} 2\alpha, \\ p\,Q &= \tfrac{1}{2} T_2 \operatorname{cosec}^2\alpha - S \operatorname{cosec} 2\alpha, \\ r\,R &= T_1 - T_2 \cot^2\alpha, \end{aligned}\right\} \quad (6)$$

from equation (3), while the t.s. system of equation (5) gives rise to fibre forces

$$\left.\begin{aligned} p\,P &= \tfrac{1}{2} T_1 \sec^2\alpha + S \operatorname{cosec} 2\alpha, \\ q\,Q &= -T_1 \tan^2\alpha + T_2, \\ p\,R &= \tfrac{1}{2} T_1 \sec^2\alpha - S \operatorname{cosec} 2\alpha. \end{aligned}\right\} \quad (7)$$

Now, sheet having three fibre-directions is elastically isotropic when the differences in angle between the fibre directions are $\pm 60^\circ$, while the numbers of fibres aligned in these three directions are the same (see equation (81), Appendix A). Thus

$$\beta = \alpha + 60^\circ, \quad \gamma = \alpha + 120^\circ, \quad p = q = r; \tag{8}$$

suppose the angles defined so that $0 < \alpha \leq 60^\circ$. Such sheet is not isotropic in all respects since its strength, for example, varies according to direction; it is however, usually referred to as 'isotropic', and this will be followed in the present Paper. The fibre forces P, Q and R are then given by

$$\left.\begin{aligned} 3p\,P &= (T_1 + T_2) + 2(T_1 - T_2)\cos 2\alpha + 4S \sin 2\alpha, \\ 3p\,Q &= (T_1 + T_2) + 2(T_1 - T_2)\cos(2\alpha + 120^\circ) + 4S \sin(2\alpha + 120^\circ), \\ 3p\,R &= (T_1 + T_2) + 2(T_1 - T_2)\cos(2\alpha + 240^\circ) + 4S \sin(2\alpha + 240^\circ), \end{aligned}\right\} \tag{9}$$

from equation (3). When isotropic sheet is aligned in an l.s. manner, that is when

$$\alpha = 60^\circ, \quad \beta = 120^\circ, \quad \gamma = 180^\circ, \quad p = q = r, \tag{10}$$

the fibre forces are given by

$$\left.\begin{aligned} 3p\,P &= 2T_2 + 2\sqrt{3}\,S, \\ 3p\,Q &= 2T_2 - 2\sqrt{3}\,S, \\ 3p\,R &= 3T_1 - T_2 \end{aligned}\right\} \tag{11}$$

from equation (6). The t.s. isotropic system, defined by

$$\alpha = 30^\circ, \quad \beta = 90^\circ, \quad \gamma = 150^\circ, \quad p = q = r, \tag{12}$$

gives rise to fibre forces

$$\left.\begin{aligned} 3p\,P &= 2T_1 + 2\sqrt{3}\,S, \\ 3p\,Q &= -T_1 + 3T_2, \\ 3p\,R &= 2T_1 - 2\sqrt{3}\,S. \end{aligned}\right\} \tag{13}$$

The applied load is carried in the fibres as either tension or compression. The tensile force in any fibre will clearly be less than the ultimate strength U of an average fibre and the compressive force will be greater than some other value. The restriction

$$-\mu U < \text{tension in an average fibre} < U \qquad (14)$$

($\mu < 1$) is therefore introduced. The ability of fibres to take compression is complicated and differs according to fibre material, matrix and form of construction; an individual fibre may develop a high strength in tension but, having a low bending stiffness due to its innate thinness, will not be able to demonstrate any appreciable strength in compression on account of instability. When set in a matrix, however, fibre behaviour in compression will be similar to that of a beam on an elastic foundation and individual fibre-stability will be improved. An assemblage of fibres laminated in a matrix material will exhibit other tendencies; a fibre in compression which has laminae of fibres in tension adjacent to it may be expected to derive some stabilising influence from these. It is thus clear that, if an optimisation is to be carried out, some overall simplification must be made and it is assumed that μ, defined above, is a constant. There is thus some lower limit, derived from unspecified strength or stability considerations, on the compression which can be developed in any single fibre.

The mass of fibre per unit area of sheet is

$$(p + q + r)\, A\sigma,$$

where A is the cross-sectional area of an average fibre and σ is the density of the fibre material. Thus, in what follows a non-dimensional 'density' of fibre per unit area of sheet,

$$\rho = \frac{U}{T}(p + q + r), \qquad (15)$$

will be used, T being a typical applied force, Other dimensional constants of the sheet follow; in fact

$$\left.\begin{aligned} &\text{Mass of fibre per unit area of sheet} = \frac{\sigma A T \rho}{U}, && \text{(a)} \\ &\text{Ultimate strength of fibre material} = \frac{U}{A}. && \text{(b)} \end{aligned}\right\} \qquad (16)$$

It is relevant to consider also the strength properties of sheet fabricated from solid material having the same properties as the fibres in order to make like-with-like comparisons between the properties of reinforced and sheet materials. Yield in a solid sheet of thickness h which is governed by the Mises-Hencky yield criterion[7] is given by

$$N_x^2 - N_x N_y + N_y^2 + 3N_{xy}^2 = h^2 U^2 A^{-2}$$

(cf. equation (16b)). The thinnest sheet able to carry the load system of equation (1) thus has density given by

$$\rho = \frac{1}{T}\sqrt{T_1^2 - T_1 T_2 + T_2^2 + 3S^2}, \qquad (17)$$

from equation (16a).

Stiffness of reinforced sheet is not specifically used in the analysis of this Report; for completeness, however, the elastic constants of the fibre-systems above are derived in Appendix A.

3 OPTIMUM ARRANGEMENTS FOR UNIAXIAL TENSION AND SYMMETRIC SHEAR VARIATION

Expressions having been established for the load carried in any fibre-direction the optimum arrangement of fibre needed to carry given uniform load systems may be considered. The applied load-system first considered is

$$\left.\begin{aligned} &0 < T_1 < T, \\ &T_2 = 0, \\ &-\lambda T < S < \lambda T \end{aligned}\right\} \qquad (18)$$

(cf. equation (1)); this corresponds to a rectangular load-envelope in the (N_x, N_{xy}) plane, symmetric with respect to the N_x-axis. The optimisation carried out is that of minimising the density ρ subject to the constraint that, for all the applied load fields of equation (18), the restriction of equation (14) on fibre forces is observed at all points on the load envelope.

Since the applied load system of equation (18) is symmetric with respect to the Ox and Oy axes, attention is restricted to symmetric fibre arrangements.

3.1 General optimum arrangement

If the l.s. system of Section 2 is considered, then

$$\left.\begin{aligned} p\,P &= -\,p\,Q = S \operatorname{cosec} 2\alpha, \\ r\,R &= T_1, \end{aligned}\right\} \qquad (19)$$

from equations (4), (6) and (18). The (P, Q) and R-fibre systems thus carry shear and tension independently and may be independently optimised.

Since the R-fibres are always in tension, it is easily seen that

$$\min (r) = \frac{T}{U},$$

corresponding to $T_1 = T$ and $R = U$. One of the P and Q fibre-systems will be in compression, and for any given α it follows that

$$\min (p) = \frac{\lambda T}{\mu U} \operatorname{cosec} 2\alpha$$

corresponding to $S = \lambda T$ and $Q = -\mu U$ (or $S = -\lambda T$ and $P = -\mu U$). The lowest fibre-density for a given value of α is thus

$$\min (\rho) = \frac{U}{T} \min (2p + r) = 1 + \frac{2\lambda}{\mu} \operatorname{cosec} 2\alpha.$$

The minimum density for all values of α occurs when $\alpha = 45°$; the fibre orientation and distribution are then given by

$$\rho_o = 1 + \frac{2\lambda}{\mu}, \quad \alpha_o = 45°, \quad (p_o, q_o, r_o) = \frac{T}{U}\left(\frac{\lambda}{\mu}, \frac{\lambda}{\mu}, 1\right). \qquad (20)$$

This best arrangement is determined by limiting tension in the R-fibres at the maximum value of N_x and limiting compression in the (P, Q) fibres at the maximum shear N_{xy}.

In the t.s. system of Section 2 the fibre forces are

$$\left.\begin{aligned} p\,P &= \tfrac{1}{2} T_1 \sec^2 \alpha + S \operatorname{cosec} 2\alpha, \\ q\,Q &= -\,T_1 \tan^2 \alpha, \\ p\,R &= \tfrac{1}{2} T_1 \sec^2 \alpha - S \operatorname{cosec} 2\alpha, \end{aligned}\right\} \qquad (21)$$

from equations (5), (7) and (18). The Q-fibres are always in compression, and it follows that

$$\min(q) = \frac{T}{\mu U} \tan^2 \alpha, \tag{22}$$

corresponding to $T_1 = T$ and $Q = -\mu U$. If $S \geq 0$, the minimum value of p will be determined either by having enough fibres to resist the maximum tensile P (when $T_1 = T$, $S = \lambda T$) or the maximum compressive R (when $T_1 = 0$, $S = \lambda T$). It follows that

$$\min (p) = \frac{T}{U} \max \left\{ \tfrac{1}{2} \sec^2 \alpha + \lambda \operatorname{cosec} 2\alpha, \frac{\lambda}{\mu} \operatorname{cosec} 2\alpha \right\},$$

whence

$$\rho = \frac{U}{T} \min (2p + q) = \begin{cases} f_1(\alpha) & \text{when } 0 < \alpha < \phi_1, \\ f_2(\alpha) & \text{when } \phi_1 < \alpha < 90^\circ, \end{cases} \tag{23}$$

where

$$\left.\begin{aligned} \mu f_1(\alpha) &= 2\lambda \operatorname{cosec} 2\alpha + \tan^2 \alpha, \\ \mu f_2(\alpha) &= \mu \sec^2 \alpha + 2\lambda\mu \operatorname{cosec} 2\alpha + \tan^2 \alpha \end{aligned}\right\} \tag{24}$$

and

$$\tan \phi_1 = \frac{\lambda}{\mu}(1 - \mu). \tag{25}$$

If the restriction that $S \geq 0$ is removed, equation (23) still holds since the roles of the P and R-fibres in resisting tension and compression are reversed. Each of the functions $f_1(\alpha)$ and $f_2(\alpha)$ has a single minimum for $0 < \alpha < 90^\circ$; these are α_1 and α_2 respectively, defined by

$$\left.\begin{aligned} \tan^2 \alpha_1 \tan 2\alpha_1 &= \lambda \\ \text{and} \qquad \tan^2 \alpha_2 \tan 2\alpha_2 &= \frac{\lambda\mu}{1 + \mu}. \end{aligned}\right\} \tag{26}$$

Since $\mu < 1$, $\alpha_2 < \alpha_1 < 45^\circ$.

The minimum value of the density $\rho(\alpha)$, defined by equation (23), depends on the relative magnitudes of the angles α_1, α_2 and ϕ_1; it can be shown that this minimum is achieved at the median of these angles; if the median is either α_1 or α_2 the minimum is a conventional one (i.e. corresponds to a vanishing first derivative) whereas if it is at ϕ_1 the minimum lies at the intersection of the two functions $f_1(\alpha)$ and $f_2(\alpha)$. The minimum density for all t.s. systems depends on the shear-ratio λ, and is given by

$$\rho = \begin{cases} f_1(\alpha_1), \quad \alpha = \alpha_1 & \text{if } 0 < \lambda < \lambda_1, \quad \text{(a)} \\ \dfrac{\lambda^2 (1-\mu)}{\mu^3} + \dfrac{1}{1-\mu}, \quad \alpha = \phi_1 & \text{if } \lambda_1 < \lambda < \lambda_2, \quad \text{(b)} \\ f_2(\alpha_2), \quad \alpha = \alpha_2 & \text{if } \lambda > \lambda_2 \quad \text{(c)} \end{cases} \tag{27}$$

with, in all cases,

$$q = \frac{T \tan^2 \alpha}{U\mu}, \quad 2p = \frac{T}{U}\rho - q \tag{27d}$$

and

$$\lambda_1 = \frac{\mu^2}{(1-\mu)\sqrt{2-\mu^2}}, \quad \lambda_2 = \frac{\mu\sqrt{\mu}}{(1-\mu)\sqrt{2-\mu}}. \tag{28}$$

For small variations of the shear, the orientation in this arrangement is the *same* whatever the value of μ (cf. equations (26) and (27a)).

Now the line

$$\rho_o = 1 + \frac{2\lambda}{\mu} \tag{20 bis}$$

touches the curve

$$\rho = \frac{\lambda^2 (1-\mu)}{\mu^3} + \frac{1}{1-\mu} \tag{27b bis}$$

at the point where

$$\rho_o = \frac{1+\mu}{1-\mu}, \quad \lambda = \frac{\mu^2}{1-\mu}, \quad \tan\alpha = \mu. \tag{29}$$

Since

$$\lambda_1 < \frac{\mu^2}{1-\mu} < \lambda_2$$

the l.s. and t.s. systems which correspond to equations (20) and (27b) will have the same density for the one particular shear λ of equation (29). If $\mu = 1$ the above argument breaks down; this equality of density between the l.s. and t.s. arrangements only holds when $\mu < 1$ and is thus a consequence of the inefficiency of the fibres in resisting compression.

The l.s. and t.s. systems are the two contenders for the title of optimum arrangement. It may be shown by computation that the l.s. system of equation (20) has, in all cases, a lower density than the t.s. system of equation (27) and is therefore the true optimum. Figs.2-4 have been prepared to show the variation of optimum fibre density ρ_o with shear/tension ratio λ and to compare these optima with the best fibre densities arising from the t.s. fibre-arrangement. The fibre orientations in the t.s. system are indicated. In Fig.2, corresponding to the case when fibres are allowed to develop the same tensile and compressive load ($\mu = 1$), it is seen that the l.s. arrangement has a considerable advantage for all positive values of λ over the t.s. system. It is, of course, unlikely that the allowable compressive and tensile fibre loads will be the same, and Figs.3 and 4 correspond to values of $\mu = 0{\cdot}75$ and $\mu = 0{\cdot}5$ respectively. The l.s. arrangement is generally superior to the t.s. arrangement although, for $\mu = 0{\cdot}75$ and moderate values of the shear, the superiority is only marginal. Moreover, for the one particular value of λ already referred to (cf. equation (29)) the two alternative arrangements lead to the same fibre-density; for clarity the part of the curve corresponding to the t.s. system is omitted in this region in Figs.3 and 4.

The fraction of fibre in the optimum l.s. system of equation (20) which is aligned in the $\pm 45^\circ$ directions is shown in Fig.5 to illustrate the variation of the fraction of fibre needed to resist shear; the inclusion of $\mu = 0{\cdot}25$ shows the effect of using fibres which can only develop very low compression, considerably more fibre being needed to withstand the compressive component of any applied shear.

The elastic constants of the l.s. and t.s. systems of equation (20) and (29) are given in equations (78) and (80) of Appendix A.

3.2 Optimum isotropic arrangement

Elastically isotropic sheet subjected to the load distribution of equation (18) and aligned as a l.s. system will have fibre forces given by

$$\left.\begin{aligned} p\,P &= -\,p\,Q = 2\sqrt{3}\,S/3 \\ p\,R &= T_1, \end{aligned}\right\} \qquad (30a)$$

from equation (11). Isotropic sheet aligned in a t.s. manner and subjected to the load system of equation (18) will have fibre forces given by

$$\left.\begin{aligned} 3p\,P &= 2T_1 + 2\sqrt{3}\,S, \\ 3p\,Q &= -T_1, \\ 3p\,R &= 2T_1 - 2\sqrt{3}\,S, \end{aligned}\right\} \qquad (30b)$$

from equation (13). Optimisation of symmetric isotropic fibre arrangements thus depends on choosing the better of the l.s. and t.s. arrangements and minimising the fibre density. In either of those two arrangements the density will be determined by the need to provide sufficient fibre to resist limiting tensile and compressive forces. Thus for l.s. arrangements

$$\min(\rho) = \max\left\{3,\ 2\sqrt{3}\,\frac{\lambda}{\mu}\right\},$$

which is determined by limiting tensile R or compressive (P, Q) in equation (30a), while for t.s. arrangements

$$\min(\rho) = \max\left\{\frac{1}{\mu},\quad 2 + 2\sqrt{3}\lambda,\quad 2\sqrt{3}\,\frac{\lambda}{\mu}\right\},$$

which corresponds to limiting tensile P or compressive (Q, R) in equation (30b). The optimum isotropic arrangement will thus have density

$$\rho_o = \min\left[\max\left\{3,\ 2\sqrt{3}\,\frac{\lambda}{\mu}\right\},\ \max\left\{\frac{1}{\mu},\ 2 + 2\sqrt{3}\,\lambda,\ 2\sqrt{3}\,\frac{\lambda}{\mu}\right\}\right]. \qquad (31)$$

For comparison with the general optimum, this isotropic-optimum density is also shown in Figs.2-4 alongside the density of general optimum sheet.

It is of interest that for no applied shear ($\lambda = 0$) equation (31) gives

$$\rho_o = \begin{cases} 2 \text{ if } \mu > \frac{1}{2}, \\ \frac{1}{\mu} \text{ if } 1/3 < \mu < \frac{1}{2}, \\ 3 \text{ if } \mu < 1/3. \end{cases}$$

Hence, unless the fibres are poor in compression ($\mu < 1/3$), it is better to use the t.s. orientation of isotropic sheet to carry uniaxial tension. Thus it is better to have two fibre systems aligned at $\pm 30^\circ$ working a little inefficiently by carrying an increased component of the tensile load than it

is to have only one fibre system at 180° which carries the full tensile load efficiently with the other two fibre systems not contributing at all. The restriction on μ arises since with fibres aligned at ±30° the role of the transverse fibres is to resist compression.

A further parameter relevant to the possible use of reinforced composites is the ratio of the density of optimum to isotropic sheet for any particular load envelope; this ratio gives an indication of the efficiency of isotropic sheet. Fig.6 shows this variation for sheets in which $\mu = 1{\cdot}0$, $0{\cdot}75$ and $0{\cdot}5$. Now, when $\lambda = \frac{1}{2}\mu\sqrt{3}$,

$$\frac{\text{Optimum } \rho}{\text{Optimum isotropic } \rho} = \frac{1+\sqrt{3}}{3} = 0{\cdot}91,$$

from equations (20) and (31); this is independent of μ. It is seen in Fig.6 that the density ratio varies between $0{\cdot}5$ and the above value of $0{\cdot}91$ for all sheets for which $\mu > \frac{1}{2}$. For sheets in which $\mu < \frac{1}{2}$ the ratio falls below $0{\cdot}5$ but these are not specifically considered. It is of interest that when $\lambda = \frac{1}{2}\mu\sqrt{3}$ the optimum density is only $0{\cdot}91$ of the best isotropic density. In fact, for this particular value of λ,

$$(p_o,\ q_o,\ r_o) = \frac{T}{U}(0{\cdot}866,\ 0{\cdot}866,\ 1)$$

in the optimum arrangement aligned at (±45°, 180°), while

$$(p_o,\ q_o,\ r_o) = \frac{T}{U}(1,\ 1,\ 1)$$

is the isotropic arrangement aligned at (±60°, 180°). Thus the only inefficiency in the isotropic arrangement is that of aligning fibres at ±60° rather than at ±45° in addition to those aligned at 180°, and this is slight.

3.3 Density of solid sheet

The optimum arrangement may also be compared with sheet fabricated from solid material; the minimum density of such sheet is

$$\rho = \sqrt{1+3\lambda^2}, \qquad (32)$$

from equations (17) and (18). This density is also shown in Figs.2-4 to facilitate comparison with the fibre-reinforced sheets already considered.

The ability possessed by solid material to withstand complex loading without the same increase in density as fibre-reinforced material is illustrated; it should be borne in mind that μ is a property of the fibre-matrix composite rather than a constant of the material.

Fig.7 shows the ratio of the density of solid to optimum sheet for various values of μ; this ratio gives the efficiency of optimum sheet when regarded as a method of construction. The value $\mu = 0{\cdot}25$ has been included to show the effect of restriction of the compressive load allowed in the fibres. As might be expected, in all cases the density ratio has an upper limit of unity corresponding to simple tension. Even if the compressive fibre load is unrestricted (i.e. $\mu = 1$) the efficiency can fall to 0·65; further restrictions on compressive load imply, in general, lower efficiencies and the lowest value illustrated is one of 0·21 when $\mu = 0{\cdot}25$. These figures, of course, must be interpreted with care if used in assessing a practical application; so far as the composite is concerned they relate solely to the weight of fibre and this is assumed to be working with full efficiency. Actual composite efficiencies will be much less than those quoted above; a 'loading' factor in the region of 0·59 (for low density fibres) to 0·66 (for higher density fibres) is probably reasonable if accounting roughly for the presence of a resinous matrix material at a volume fraction of 0·5, while a further 'loading' will exist to account for the loss in fibre efficiency; Porter[8], for example, quotes a fibre efficiency of 0·68 for cross-plied continuous-fibre composites.

4 OPTIMUM ARRANGEMENTS FOR BIAXIAL TENSION AND SYMMETRIC SHEAR VARIATION

The example of Section 3 having been concerned with combined uniaxial tension and shear, a problem in which biaxial tension exists is next considered. The optimisation is carried out for the applied load-envelope

$$\left.\begin{aligned} 0 < T_1 < T, \\ 0 < T_2 < \tfrac{1}{2}T, \\ -\lambda T < S < \lambda T. \end{aligned}\right\} \qquad (33)$$

The load-envelope is a rectangular solid in the (N_x, N_y, N_{xy}) load-space. Since the loading is symmetric, attention is again restricted to the l.s. and t.s. fibre-arrangements of Section 2.

4.1 General optimum arrangements

The fibre forces in the l.s. system are given by equation (6), from which it follows that the minimum densities p and r for any particular orientation α are given by

$$\left.\begin{aligned} p &= \frac{T}{U} \max\left\{\frac{1}{4}\operatorname{cosec}^2\alpha + \lambda \operatorname{cosec} 2\alpha,\ \frac{\lambda}{\mu}\operatorname{cosec} 2\alpha\right\} \\ \text{and} \qquad r &= \frac{T}{U} \max\left\{1,\ \frac{1}{2\mu}\cot^2\alpha\right\}, \end{aligned}\right\} \tag{34}$$

the terms on the right corresponding to limiting tensile P, compressive Q and limiting tensile and compressive R respectively (when $S > 0$). The form taken by the density thus depends on the larger of the expressions on the right of equation (34); it follows that

$$\rho = \left\{\begin{array}{ll} g_1(\alpha) & \text{when } 0 < \alpha < \theta_1 \\ \frac{3}{2} + g_2(\alpha) & \text{when } \theta_1 < \alpha < \theta_2 \\ 1 + \frac{2\lambda}{\mu}\operatorname{cosec} 2\alpha & \text{when } \theta_2 < \alpha \end{array}\right\} \text{if } \lambda < \lambda_3 \tag{35a}$$

and

$$\rho = \left\{\begin{array}{ll} g_1(\alpha) & \text{when } 0 < \alpha < \theta_2 \\ \frac{1}{\mu} g_2(\alpha) & \text{when } \theta_2 < \alpha < \theta_1 \\ 1 + \frac{2\lambda}{\mu}\operatorname{cosec} 2\alpha & \text{when } \theta_1 < \alpha \end{array}\right\} \text{if } \lambda > \lambda_3, \tag{35b}$$

where

$$\left.\begin{aligned} 2\mu\, g_1(\alpha) &= \mu \operatorname{cosec}^2\alpha + 4\lambda\mu \operatorname{cosec} 2\alpha + \cot^2\alpha, \\ 2 g_2(\alpha) &= \cot^2\alpha + 4\lambda \operatorname{cosec} 2\alpha, \end{aligned}\right\} \tag{36a}$$

and

$$\cot\theta_1 = \sqrt{2\mu}, \quad \cot\theta_2 = \frac{2\lambda(1-\mu)}{\mu}, \quad \lambda_3 = \frac{\mu\sqrt{\mu}}{(1-\mu)\sqrt{2}}. \tag{36b}$$

The functions $g_1(\alpha)$ and $g_2(\alpha)$ each have single minima for $0 < \alpha < 90°$; they are α_1' and α_2', where

$$\left.\begin{aligned} &\cot^2 \alpha_1' + \frac{2\lambda\mu}{1+\mu} \cot 2\alpha_1' = 0 \\ \text{and} \qquad &\cot^2 \alpha_2' + 2\lambda \cot 2\alpha_2' = 0, \end{aligned}\right\} \tag{37}$$

whence it follows that

$$90^\circ > \alpha_1' > \alpha_2' > 45^\circ.$$

Since $1 + \frac{2\lambda}{\mu}$ cosec 2α has a minimum when $\alpha = 45^\circ$, it can be shown that the minimum of the density function, as defined by equation (35), depends on the relative magnitudes of the angles α_1', α_2', 45°, θ_1 and θ_2, the minimum being achieved at the median of these angles. If the median is α_1', α_2' or 45° then the minimum is conventional (i.e. corresponds to a vanishing derivative) whereas if it is θ_1 or θ_2 it lies at the intersection of two functions. The minimum density is then, in general, given by

$$\rho_o = \left\{\begin{aligned} &1 + \frac{2\lambda}{\mu} && \text{if } \alpha_o = 45^\circ \text{ is the median,} \\ &g_1(\alpha_1') && \text{if } \alpha_o = \alpha_1' \text{ is the median,} \end{aligned}\right\} \tag{38a}$$

$$\rho_o = \left\{\begin{aligned} &\frac{3}{2} + g_2(\alpha_2') && \text{if } \alpha_o = \alpha_2' \text{ is the median} \\ &\frac{\lambda(1+2\mu)}{\mu\sqrt{2\mu}} + \mu + \frac{3}{2} && \text{if } \alpha_o = \theta_1 \text{ is the median} \\ &\frac{2\lambda^2(1-\mu)}{\mu^2} + \frac{1}{2(1-\mu)} + 1 && \text{if } \alpha_o = \theta_2 \text{ is the median} \end{aligned}\right\} \text{ and } \lambda < \lambda_3, \tag{38b}$$

$$\rho_o = \left\{\begin{aligned} &\frac{1}{\mu} g_2(\alpha_2') && \text{if } \alpha_o = \alpha_2' \text{ is the median} \\ &1 + \frac{\lambda(1+2\mu)}{\mu\sqrt{2\mu}} && \text{if } \alpha_o = \theta_1 \text{ is the median} \\ &\frac{1}{2(1-\mu)} + \frac{2\lambda^2(1-\mu)}{\mu^3} && \text{if } \alpha_o = \theta_2 \text{ is the median} \end{aligned}\right\} \text{ and } \lambda > \lambda_3. \tag{38c}$$

Equations (38a,b,c) enable the minimum density to be found in any particular case. A simplification ensues if attention is restricted to sheets for which $\mu > \frac{1}{2}$, since then $\theta_1 < 45^\circ$ and

$$\alpha_1' > \alpha_2' > 45^\circ > \theta_1$$

(cf. equation (37) and the remarks following). Depending on the magnitude of θ_2, only α_2', 45° or θ_2 can then be the median, and the following expressions for the minimum density are derived;

$$\rho_o = \begin{cases} \frac{3}{2} + g_2(\alpha_2'), & \alpha_o = \alpha_2' \text{ when } 0 < \lambda < \lambda_4, \\ \frac{2\lambda^2(1-\mu)}{\mu^2} + \frac{1}{2(1-\mu)} + 1, & \alpha_o = \theta_2 \text{ when } \lambda_4 < \lambda < \lambda_5, \\ 1 + \frac{2\lambda}{\mu}, & \alpha_o = 45^\circ \text{ when } \lambda > \lambda_5, \end{cases} \quad (\mu > \tfrac{1}{2}) \quad \begin{matrix} \text{(a)} \\ \text{(b)} \\ \text{(c)} \end{matrix} \qquad (39)$$

where

$$\lambda_4 = \frac{\mu\sqrt{\mu}}{2(1-\mu)\sqrt{2-\mu}}, \quad \lambda_5 = \frac{\mu}{2(1-\mu)}. \qquad (40)$$

It is noteworthy that, for small values of the shear-ratio λ, the orientation and density in this l.s. arrangement are independent of μ (cf. equations (37) and (39a)).

In a t.s. system, the fibre forces are given by equation (7); it follows that the minimum densities p and q for any particular orientation α are given by

$$\left.\begin{aligned} p &= \frac{T}{U} \max\left\{\tfrac{1}{2}\sec^2\alpha + \lambda \operatorname{cosec} 2\alpha,\ \frac{\lambda}{\mu}\operatorname{cosec} 2\alpha\right\} \\ \text{and} \qquad q &= \frac{T}{U} \max\left\{\tfrac{1}{2},\ \frac{1}{\mu}\tan^2\alpha\right\}, \end{aligned}\right\} \qquad (41)$$

the terms on the right corresponding, when $S > 0$, to limiting tensile P, compressive R and tensile and compressive Q respectively. It follows that the lowest density is

$$\rho = \left\{ \begin{array}{ll} \frac{1}{2} + \frac{2\lambda}{\mu} \operatorname{cosec} 2\alpha & \text{when } 0 < \alpha < \phi_1 \\ \frac{3}{2} + \mu f_1(\alpha) & \text{when } \phi_1 < \alpha < \phi_2 \\ f_2(\alpha) & \text{when } \phi_2 < \alpha \end{array} \right\} \text{ if } \lambda < \lambda_3 \qquad (42a)$$

and

$$\rho = \left\{ \begin{array}{ll} \frac{1}{2} + \frac{2\lambda}{\mu} \operatorname{cosec} 2\alpha & \text{when } 0 < \alpha < \phi_2 \\ f_1(\alpha) & \text{when } \phi_2 < \alpha < \phi_1 \\ f_2(\alpha) & \text{when } \phi_1 < \alpha \end{array} \right\} \text{ if } \lambda > \lambda_3, \qquad (42b)$$

where ϕ_1, $f_1(\alpha)$ and $f_2(\alpha)$ are defined by equations (24) and (25) and

$$\tan \phi_2 = \sqrt{\frac{\mu}{2}} \, . \qquad (43)$$

The minimum density corresponding to equation (42) is achieved at the median of the angles α_1, α_2, $45°$, ϕ_1 and ϕ_2; it has already been remarked that $0 < \alpha_2 < \alpha_1 < 45°$. It follows that

$$\rho = \left\{ \begin{array}{ll} \frac{1}{2} + \frac{2\lambda}{\mu} & \text{if } 45° \text{ is the median,} \\ f_2(\alpha_2) & \text{if } \alpha_2 \text{ is the median,} \end{array} \right\} \qquad (44a)$$

$$\rho = \left\{ \begin{array}{ll} \frac{3}{2} + \mu f_1(\alpha_1) & \text{if } \alpha_1 \text{ is the median} \\ \frac{\lambda^2(1-\mu)}{\mu^2} + \frac{1}{1-\mu} + \frac{1}{2} & \text{if } \phi_1 \text{ is the median} \\ \frac{\lambda(2+\mu)}{\sqrt{2\mu}} + \frac{1}{2}\mu + \frac{3}{2} & \text{if } \phi_2 \text{ is the median} \end{array} \right\} \text{and } \lambda < \lambda_3, \qquad (44b)$$

$$\rho = \left\{ \begin{array}{ll} f_1(\alpha_1) & \text{if } \alpha_1 \text{ is the median} \\ \dfrac{\lambda^2}{\mu^3}(1-\mu) + \dfrac{1}{1-\mu} & \text{if } \phi_1 \text{ is the median} \\ \dfrac{\lambda(2+\mu)}{\mu\sqrt{2\mu}} + \dfrac{1}{2} & \text{if } \phi_2 \text{ is the median} \end{array} \right\} \text{and } \lambda > \lambda_3. \quad (44c)$$

The two contenders for the title of optimum system are thus the l.s. and t.s. systems whose densities are given by equations (38) and (44) respectively. Computation shows that, of these two systems, the l.s. one leads in general to a lower density and is therefore the true optimum. Figures 8-10 show the variation of optimum fibre density ρ_o for fibre systems in which $\mu = 1{\cdot}0$, $0{\cdot}75$ and $0{\cdot}5$ respectively; the comparison of the optimum density with the higher density arising from the t.s. arrangement is also made in these figures.

When $\mu < 1$, as in Section 3.1, at one particular value of the shear-ratio the l.s. and t.s. systems give rise to the same density. This is again a consequence of the compressive inefficiency of the fibres; when $\mu > 0{\cdot}5$, this equality occurs when

$$\lambda = \frac{\mu^2}{1-\mu}.$$

The optimum l.s. density near this value of λ is

$$\rho_o = 1 + \frac{2\lambda}{\mu} \qquad (39c) \text{ bis}$$

and the density of the t.s. system is

$$\rho = \frac{1}{1-\mu} + \frac{\lambda^2}{\mu^3}(1-\mu); \qquad (44c) \text{ bis}$$

referring to equation (29) and the preceding remarks, the local behaviour here is seen to be exactly the same as that for uniaxial tension in Section 3.1. The density and orientation here are thus also given by equation (29). In Figs.9 and 10 the part of the t.s. density curve in this region is omitted.

While the density of the l.s. arrangement is, in general, lower than that of the t.s. arrangement, for $\mu = 0{\cdot}75$ (Fig.9) and moderate shear the superiority is only marginal. For small shears it can be seen that the optimum fibre arrangement is independent of μ; it is the ability of the fibres to carry tensile load which determines the arrangement and only for larger variations of the shear do compressive fibre forces have an influence. The optimum system is again found to be the arrangement having one fibre-direction aligned parallel to the applied tension which is allowed the larger variation; this was also the case for the fibre-arrangement corresponding to uniaxial tension in Section 3.1.

When $\lambda = 0$, the optimum angle of fibre orientation is 90° and corresponds to two, rather than three, fibre directions aligned in the direction of the two applied tensions. For $\mu = 1$ the variation of α is indicated in Fig.8. When $0{\cdot}5 < \mu < 1$, the variation with λ initially follows that of Fig.8 until $\lambda = \lambda_4$; for larger shears the orientation reaches the constant value of 45° at the point indicated in Figs.9 and 10, the optimum density then varying linearly while the optimum distribution is the same as that for uniaxial tension in Section 3.1 (see equations (20) and (39c)).

The optimum fibre densities p_o and r_o also follow from equation (34); when $\mu > 0{\cdot}5$

$$r_o = \frac{T}{U}, \quad 2p_o = \frac{T}{U}\rho_o - r_o, \tag{45}$$

ρ_o being given by equation (39).

The elastic constants of the above fibre-systems are given in Appendix A.

4.2 Optimum isotropic arrangements

The fibre forces in l.s. or t.s. sheet will be given by equations (11) and (13) respectively. When subjected to the symmetrically varying load distribution of equation (33) the optimum density is given by the requirement that just sufficient fibre must be provided for no fibre to carry greater than limiting load. In the l.s. arrangement this gives a minimum density of

$$\max\left\{1 + 2\lambda\sqrt{3}, \quad 2\sqrt{3}\,\frac{\lambda}{\mu}, \quad 3, \quad \frac{1}{2\mu}\right\}$$

while in the t.s. arrangement the minimum density is

$$\max\left\{2 + 2\lambda\sqrt{3},\ \frac{3}{2},\ \frac{1}{\mu},\ 2\sqrt{3}\frac{\lambda}{\mu}\right\}.$$

The optimum is the minimum of these and

$$\rho_o = \min\left[\max\left\{1 + 2\lambda\sqrt{3},\ 2\sqrt{3}\frac{\lambda}{\mu},\ 3,\ \frac{1}{2\mu}\right\},\ \max\left\{2 + 2\sqrt{3}\lambda,\ \frac{1}{\mu},\ 2\sqrt{3}\frac{\lambda}{\mu}\right\}\right]. \quad \ldots\ (46)$$

For comparison with the density of the general optimum configuration this isotropic optimum density is also shown in Figs.9-10.

For zero applied shear ($\lambda = 0$), equation (46) gives

$$\rho_o = 2 \text{ if } \mu > 0{\cdot}5,$$

corresponding to the t.s. alignment. Thus, for sheets having sufficiently good compressive properties ($\mu > 0{\cdot}5$) the better alignment of isotropic sheet to carry the biaxial tension of equation (33) when $\lambda = 0$ is the t.s. arrangement in which fibres are aligned at $\pm 30°$ to the direction of the larger tension; this is analogous to the behaviour of isotropic sheet under uniaxial tension in Section 3.2.

Fig.11 has been prepared to show the ratio of the optimum density to the optimum isotropic density for sheets in which $\mu = 1{\cdot}0$, $0{\cdot}75$ and $0{\cdot}5$. Since for small values of λ the optimum isotropic density is independent of μ, the variation for $\mu = 0{\cdot}75$ and $\mu = 0{\cdot}5$ is shown only when it deviates from the curve for $\mu = 1$. For biaxial tension alone (i.e. when $\lambda = 0$) the density ratio is $0{\cdot}75$, while

$$\frac{\text{Optimum } \rho}{\text{Optimum isotropic } \rho} = \frac{1 + \frac{2\lambda}{\mu}}{\frac{2\lambda}{\mu}\sqrt{3}} \to 0{\cdot}58 \text{ as } \lambda \to \infty.$$

In view of the way in which the load envelope has been specified, $\lambda \to \infty$ merely corresponds to no biaxial tension rather than to an infinite shear. The maximum value of the density ratio depends on μ; thus, when $\mu = 1$ and $0{\cdot}75$ the optimum density varies between $0{\cdot}58$ and $0{\cdot}99$ of the density of the best isotropic sheet. However, isotropic sheet in which $\mu = 0{\cdot}5$ does not achieve the same efficiency.

The maximum value 0·99 of the density-ratio occurs when $\lambda = 0{\cdot}58$; at this particular λ

$$(p_o, q_o, r_o) = \frac{T}{U}(0{\cdot}99, 0{\cdot}99, 1)$$

in the optimum arrangement which is aligned at $(\pm 56°, 180°)$, while

$$(p_o, q_o, r_o) = \frac{T}{U}(1, 1, 1)$$

in the isotropic arrangement which is aligned at $(\pm 60°, 180°)$. The only inefficiency in the isotropic arrangement arises from aligning fibres at $\pm 60°$ rather than $\pm 56°$; the resulting difference in density is only slight.

4.3 Density of solid sheet

The optimum arrangement of Section 4.1 may also be compared with the density of solid sheet; the minimum density of such sheet is

$$\rho = \tfrac{1}{2}\sqrt{3 + 12\,\lambda^2}; \qquad (47)$$

from equations (17) and (33). To enable comparison to be made with the reinforced sheets already considered this density is also shown in Figs.8-10.

The direct comparison between optimum reinforced sheet and solid sheet is made in Fig.12, where the efficiency of optimum sheet is shown as a density-ratio. The value $\mu = 0{\cdot}25$ has been included to illustrate the effect of fall-off in compressive fibre-performance, the optimum fibre density being determined from equation (38). In all cases, the efficiency which corresponds to biaxial tension alone (i.e. $\lambda = 0$) is 0·58 since material has to be provided in reinforced sheet to withstand each component of the tension separately, whereas in solid sheet this is not so. For very large shear-ratios ($\lambda \to \infty$) the efficiency is the same as for uniaxial tension in Section 3.3; a minimum efficiency again exists, and varies between 0·43 (when $\mu = 1$) and 0·20 (when $\mu = 0{\cdot}25$). As was emphasised before in Section 3.3 these efficiencies should be interpreted with care.

5 OPTIMUM ARRANGEMENTS FOR UNIAXIAL TENSION AND ASYMMETRIC SHEAR VARIATION

The optimisation for uniaxial tension combined with shear varying between equal positive and negative limits was considered in Section 3.

In the wing skin of an aircraft the shear, deriving from wing torsion, is likely to be greater when arising from nose-up twisting than when derived from nose-down twisting, and in this case there would be larger limits on positive shear than on negative shear. Accordingly the optimisation is here carried out for the applied load system

$$\left.\begin{aligned} 0 < T_1 < T, \\ T_2 = 0, \\ 0 < S < \lambda T, \end{aligned}\right\} \qquad (48)$$

which is asymmetric in character and may be expected to give rise to asymmetric systems of reinforcement. The load-envelope in the (N_x, N_{xy}) plane is in this case rectangular and has no symmetry about either axis. The applied load of equation (48) is chosen to illustrate the principles involved, the lower bound of zero on the shear being taken to simplify the analysis.

5.1 General optimum arrangement

The fibre-forces are given by

$$\left.\begin{aligned} p\,P \sin(\beta - \alpha) \sin(\gamma - \alpha) &= T_1 \sin\gamma \sin\beta - S \sin(\gamma + \beta), \\ q\,Q \sin(\gamma - \beta) \sin(\beta - \alpha) &= S \sin(\alpha + \gamma) - T_1 \sin\alpha \sin\gamma, \\ r\,R \sin(\gamma - \alpha) \sin(\gamma - \beta) &= T_1 \sin\beta \sin\alpha - S \sin(\alpha + \beta), \end{aligned}\right\} \qquad (49)$$

from equations (3) and (48). Depending on a number of inequalities between α, β and γ, the three fibre densities p, q and r can be minimised separately to be just sufficient to carry the applied load of equation (48). These expressions are given in equations (83)-(85) of Appendix B and lead to a general definition of the density $\rho(\alpha, \beta, \gamma)$. The optimum fibre density follows if the values of (α, β, γ) which make ρ an absolute minimum are then found. In view of the numerous inequalities involved (cf. equations (83)-(85)) it is clear that the problem of minimising $\rho(\alpha, \beta, \gamma)$ will be difficult analytically and resort to computational minimisation techniques will be needed at an early stage. However, the previous analysis provides a useful guide; in each of Sections 3.1 and 4.1 where the shear was allowed to vary between equal positive and negative limits, two alternative fibre arrangements contended

for the title of optimum. Each arrangement corresponded to a local minimum of the density, considered as a function of fibre orientation, and the absolute minimum was decided by computation. A similar situation will probably exist in the present case and local minima of $\rho(\alpha, \beta, \gamma)$ will exist, the absolute minimum being decided computationally.

Possible local minima of ρ are thus sought; since the optimum solutions were found in Sections 3.1 and 4.1 with $\gamma = 180^\circ$, the possibility of at least a local minimum for $\gamma = 180^\circ$ is considered. If this is assumed then the fibre densities are

$$\left.\begin{aligned} \frac{U}{T} p &= \frac{\lambda \sin\beta}{\sin\alpha \sin(\beta - \alpha)}, && \text{(a)} \\ \frac{U}{T} q &= \frac{\lambda \sin\alpha}{\mu \sin\beta \sin(\beta - \alpha)}, && \text{(b)} \\ \frac{U}{T} r &= \max\left\{1, \frac{\lambda \sin(\beta + \alpha)}{\mu \sin\alpha \sin\beta}\right\}, && \text{(c)} \end{aligned}\right\} \qquad (50)$$

from equations (83)-(85) and it has been assumed that $\sin(\gamma + \beta) < 0$, $\sin(\gamma + \alpha) < 0$ and $\sin(\alpha + \beta) > 0$. In equation (50) the densities p and q are determined entirely by the resolved tensile and compressive components respectively of the shear while the value of r is determined either by direct tension (the first term in the curly brackets of equation (50c)) or a compressive force arising from the resolved component of the shear (the second term). Now whatever the shear-ratio λ, R-fibres will have to be provided to resist direct tension; it is clearly efficient to use these fibres to the full in compression also, i.e. to take

$$\frac{\lambda \sin(\alpha + \beta)}{\mu \sin\alpha \sin\beta} = 1, \qquad (51)$$

if that is possible. Now, so far as the R-fibres are concerned, for very low shears ($\lambda << 1$) tension will be paramount and use of the fibres to the limit to carry shear in this way is unlikely to be efficient; it may be desirable, however, for shears above some value $\bar{\lambda}$. Then,

$$\cot\alpha + \cot\beta = \frac{\mu}{\lambda} \quad \text{if} \quad \lambda > \bar{\lambda}, \qquad (52)$$

from equation (51). The fibre-density is then given by

$$\rho = \frac{\lambda}{\sin(\beta - \alpha)} \left\{ \frac{\sin \beta}{\sin \alpha} + \frac{\sin \alpha}{\mu \sin \beta} \right\} + 1, \tag{53}$$

from equations (50) and (52); the minimisation of this density is an unconstrained one if $\lambda < \bar{\lambda}$ and subject to the constraint of equation (52) if $\lambda > \bar{\lambda}$.

When this minimisation is carried out it is found that

$$\bar{\lambda} = \frac{\mu \sqrt{\mu}}{1 - \mu}$$

and that ρ has a minimum when

$$\gamma = 180^\circ, \quad \beta_o = 90^\circ + \alpha_o, \tag{54a}$$

with

$$\rho_o = \frac{2\lambda}{\sqrt{\mu}} + 1, \quad \tan \alpha_o = \sqrt{\mu}, \quad (p_o, q_o, r_o) = \frac{T}{U}\left(\frac{\lambda}{\sqrt{\mu}}, \frac{\lambda}{\sqrt{\mu}}, 1\right) \text{ if } \lambda < \frac{\mu \sqrt{\mu}}{1 - \mu}, \tag{54b}$$

$$\left.\begin{aligned} \rho_o = \frac{1+\mu}{2\mu}\left(\mu + \sqrt{\mu^2 + 4\lambda^2}\right), \quad (p_o, q_o, r_o) = \frac{T}{U}\left(\lambda \cot \alpha_o, \frac{\lambda}{\mu} \tan \alpha_o, 1\right), \\ \tan 2\alpha_o = \frac{2\lambda}{\mu} \qquad \text{if } \lambda > \frac{\mu \sqrt{\mu}}{1 - \mu}. \end{aligned}\right\} \tag{54c}$$

The density has been minimised with respect to α and β while holding γ = constant = 180°. It is shown in Appendix B that equations (54a,b,c) also represent a minimum of the density when γ is allowed to vary and these equations thus represent a true local minimum.

The analysis so far has been confined to the investigation of a local minimum at $\gamma = 180^\circ$. Equations (83)-(85) of Appendix B provide a general definition of the density and this has been used in conjunction with a digital computer programme which uses Piggott's mechanisation[9] of Powell's conjugate direction method[10] of function minimisation to find optimum values of fibre density. Mechanised search procedures for finding minima employ various techniques of efficient search on general surfaces in hyperspace; the Powell method is particularly powerful in that it has quadratic convergence

near a minimum. In any procedure only local minima are found and different local minima can be recovered if different starting points are chosen. It was found that, in general, for any chosen values of (λ, μ) the fibre-density $\rho(\alpha, \beta, \gamma)$ has three local minima. Two of these local minima correspond to asymmetric values of (α, β, γ) which consistently give values of the density greater than the third local minimum which is found to occur when $\gamma = 180°$. The local minimum at $\gamma = 180°$ is recovered repeatedly, thus confirming the above analysis. The arrangement typified by equation (54a,b,c) is therefore the absolute minimum and the true optimum.

It is of interest that when $\mu = 1$ the optimum solution of equation (54b) is the same as that of equation (20) for symmetric variation of shear. The fact that asymmetric systems of reinforcement have been derived is thus a direct consequence of the assumed inefficiency of fibres in compression. Since one set of fibres resists compression only and two sets resist tension only the inefficiency can be offset by re-orientation, but this possibility was not open for the symmetric shear variation of Section 3.

It is notable that for small shears, when the compressive R-component of shear is small, the geometry of the optimum fibre distribution (cf. equation (54b)) remains constant with

$$\alpha_o = \tan^{-1}\sqrt{\mu}, \quad \beta_o = 90° + \alpha_o.$$

For larger shears, when the R-fibres are used efficiently in both tension and compression, the orthogonality of the (α_o, β_o) directions is retained, while the orientation α_o increases from the value $\alpha_o = \tan^{-1}\sqrt{\mu}$ to $\alpha_o = 45°$ when $\lambda = \infty$ (cf. equation (54c)). For values of μ close to unity (i.e. for fibres which have good compressive properties) this implies very little variation of the orientation. For example,

and
$$\left.\begin{aligned} 41° < \alpha_o < 45° \quad &\text{if} \quad \mu = 0{\cdot}75 \\ 35° < \alpha_o < 45° \quad &\text{if} \quad \mu = 0{\cdot}5 \end{aligned}\right\} \text{for } 0 < \lambda < \infty .$$

The fibre-density r_o is always determined by the need to resist tension. For small shears, the densities p_o and q_o are equal (equation (54b)) but, for large shears this is no longer so (equation (54c)); the ratio of the densities of these two shear-carrying fibre systems is

$$\frac{p_o}{q_o} = \begin{cases} 1 & \text{if } \lambda < \dfrac{\mu\sqrt{\mu}}{1-\mu}, \\ \mu \cot^2 \alpha_o & \text{if } \lambda > \dfrac{\mu\sqrt{\mu}}{1-\mu}. \end{cases}$$

This ratio remains initially constant for small shears, becoming close to μ when λ becomes large and α_o approaches $45°$. The density of the optimum fibre arrangement is shown in Figs.13-15 for sheets in which $\mu = 1{\cdot}0$, $0{\cdot}75$ and $0{\cdot}5$; the orientation α_o is indicated when $\mu = 0{\cdot}75$ and $0{\cdot}5$.

The elastic constants of the asymmetric arrangement of equation (54) are given in equation (82) of Appendix A.

5.2 Optimum isotropic arrangements

Isotropic sheet aligned in a general manner and subjected to the load distribution of equation (48) will have fibre forces given by

$$\left.\begin{aligned} 3p\,P &= T_1\{1 + 2\cos 2\alpha\} + 4S \sin 2\alpha, \\ 3p\,Q &= T_1\{1 + 2\cos(2\alpha + 120°)\} + 4S \sin(2\alpha + 120°), \\ 3p\,R &= T_1\{1 + 2\cos(2\alpha + 240°)\} + 4S \sin(2\alpha + 240°), \end{aligned}\right\} \qquad (55)$$

from equation (9). Now in equation (55) the expressions

$$1 + 2\cos 2\alpha, \quad \sin 2\alpha \quad \text{and} \quad 1 + 2\cos(2\alpha + 240°)$$

are positive for $0 < \alpha \leqslant 60°$; the expressions

$$1 + 2\cos(2\alpha + 120°) \quad \text{and} \quad \sin(2\alpha + 240°)$$

are negative for $0 < \alpha \leqslant 60°$, while

$$\sin(2\alpha + 120°) \begin{cases} \geqslant 0 & \text{if } 0 < \alpha \leqslant 30°, \\ < 0 & \text{if } 30° < \alpha \leqslant 60°. \end{cases}$$

Sufficient fibre must be provided for none of the (P, Q, R) fibres to develop limiting load in either tension or compression; it follows that, for any orientation α,

$$\rho = \max\{1 + 2\cos 2\alpha + 4\lambda \sin 2\alpha,\ 1 + 2\cos(2\alpha + 240°),\ -\frac{4\lambda}{\mu}\sin(2\alpha + 240°),\ f_3(\alpha)\} \quad \ldots\ (56a)$$

where

$$f_3(\alpha) = \begin{cases} \max\left\{\dfrac{-1 - 2\cos(2\alpha + 120°)}{\mu},\ 4\lambda \sin(2\alpha + 120°)\right\} & \text{if } 0 < \alpha \leq 30°, \\ -\dfrac{1}{\mu}\{1 + 2\cos(2\alpha + 120°) + 4\lambda \sin(2\alpha + 120°)\} & \text{if } 30° < \alpha \leq 60°. \end{cases} \quad \ldots\ (56b)$$

The particular functional form of the density depends on the implied inequalities of equation (56). Encouraged by the results of Section 5.1 it may be supposed that efficient arrangements result from choosing the orientation α to ensure equality between suitable pairs of the functions in equation (56), since this means that fibres are used to the full in both tension and compression at different points on the load-envelope. The optimum arrangement will then be found to correspond to such a point of intersection. It is most profitable to restrict further attention to sheets for which $\mu > 0{\cdot}5$; equation (56) provides a suitable definition of the density if $\mu < 0{\cdot}5$. It can then be shown that for small values of the shear ($\lambda < \lambda_6$, say) the optimum occurs when α is given by

$$1 + 2\cos(2\alpha + 240°) = 1 + 2\cos 2\alpha + 4\lambda \sin 2\alpha, \quad \text{if } \lambda < \lambda_6, \qquad (57a)$$

while for high values of the shear

$$1 + 2\cos 2\alpha + 4\lambda \sin 2\alpha = -\frac{1}{\mu}\{1 + 2\cos(2\alpha + 120°) + 4\lambda \sin(2\alpha + 120°)\}$$
$$\text{if } \lambda > \lambda_6. \qquad (57b)$$

It follows that, in general,

$$\rho_o = 1 + \frac{2\lambda + \sqrt{3}}{\sqrt{3 - 2\lambda\sqrt{3} + 4\lambda^2}}, \quad 2\alpha_o = \tan^{-1}\left(\frac{3}{\sqrt{3} - 4\lambda}\right) \text{ if } \lambda < \lambda_6, \quad \ldots\ (58a)$$

$$\rho_o = \frac{3(1-\mu) + \sqrt{48\lambda^2(1-\mu+\mu^2) + 9(1-\mu)^2}}{2(1-\mu+\mu^2)},$$

$$\alpha_o = 90^\circ - \tfrac{1}{2}\tan^{-1}\frac{2\mu - 1 + 2\lambda\sqrt{3}}{2\lambda(2\mu-1) - \sqrt{3}} + \tfrac{1}{2}\sin^{-1}\frac{1+\mu}{2\sqrt{(1+4\lambda^2)(1-\mu+\mu^2)}} \quad \text{if } \lambda < \lambda_6, \qquad \ldots\ (58b)$$

the inverse tangent being between 0° and 180°. The constant λ_6 is the positive root of

$$48\lambda^4 - 16\sqrt{3}(1+\mu)\lambda^3 + 24(2-\mu)\lambda^2 - 6\sqrt{3}(1-\mu^2)\lambda + 9(1-2\mu) = 0, \qquad (59)$$

being derived by equating the two values of ρ_o in equations (58a,b).

Figs.13-15 show, for μ = 1·0, 0·75 and 0·5, the variation of the optimum isotropic density to allow comparison with the general optimum density of Section 5.1; it may be seen in equation (58a) that this density is independent of μ for small shear-ratios λ. Fig.16 has been prepared to illustrate the ratio of the general optimum density to the optimum isotropic density. When μ = 1 the optimum density varies between 0·5 and 0·91 of the density of the best-orientated isotropic sheet, while for μ = 0·75 and 0·5 isotropic sheet is less efficient. When μ = 1 and $\lambda = \frac{1}{2}\sqrt{3}$ both the optimum and isotropic arrangements are the same as in Sections 3.1 and 3.2; the maximum density ratio, 0·91, is thus the same giving an efficient isotropic arrangement for the reasons discussed in Section 3.2. In the present case the orientation of isotropic sheet can be varied according to the amount of shear to be carried; this is illustrated in Fig.17. When μ = 1 the orientation α_o takes values between 30° and 60° while for 0·5 < μ < 1, α_o is more restricted in its variation. This arises since the compression taken in those fibres which are aligned at (α_o + 60°) must be kept within the allowable limits; the restriction is thus greater for fibres which have a restricted compressive performance. This only holds for large shears, and for small shears it may be seen that the orientation is independent of μ (cf. equation (58a)).

5.3 Density of solid sheet

The comparison between the density of optimum reinforced sheet and solid sheet may again be made; the minimum density of solid sheet is again

$$\rho = \sqrt{1+3\lambda^2} \qquad (32)\text{bis}$$

(from equations (17) and (48)), this density is the same as that of Section 3.3 since solid sheet derives no particular benefit from the asymmetry of the shear. Figs.13-15 show the density of solid sheet alongside the densities of optimum and isotropic sheets for which μ = 1·0, 0·75 and 0·5.

Fig.18 shows the density ratio of solid to optimum sheet; the pattern is broadly similar to that discussed for symmetric shear variation in Section 3.3 and illustrated in Fig.7. In the present case, however, the efficiency varies between unity and 0·65 (when μ = 1) or 0·34 (when μ = 0·25); when $\mu < 1$ the reinforced sheets derive a benefit from the asymmetry of the shear by using asymmetric reinforcement and these efficiencies are slightly better than those derived in Section 3.3.

6 OPTIMUM ARRANGEMENT FOR ARBITRARILY DIRECTED UNIAXIAL TENSION

The optimum arrangement of fibre-reinforcement needed to carry a uniaxial tension which may vary arbitrarily in direction is next considered, since this typifies the capability which is usually assumed without question in solid sheet. When arbitrarily directed applied tension is resolved along fixed axes both shear and direct components of load must exist; a minimum of three directions is thus necessary if this load is always to be carried by the fibres. Since the load envelope has no preferred direction, the optimum three-fibre arrangement will be symmetric in distribution and orientation; it will therefore be isotropic. In the context of the present Paper, it is more convenient to fix the direction of the applied tension and vary the orientation of the isotropic fibre-distribution. The fibre-loads are thus given by

$$\left.\begin{aligned} 3p\,P &= T_1\{1 + 2\cos 2\alpha\}, \\ 3p\,Q &= T_1\{1 + 2\cos(2\alpha + 120°)\}, \\ 3p\,R &= T_1\{1 + 2\cos(2\alpha + 240°)\}, \end{aligned}\right\} \qquad (60)$$

from equation (9), the applied load being governed by

$$\left.\begin{aligned} 0 < T_1 &< T, \\ T_2 &= S = 0. \end{aligned}\right\} \qquad (61)$$

The minimum density follows from ensuring that none of the (P,Q,R)-fibres exceeds limiting load for any $\alpha(0 < \alpha \leq 60^\circ)$. From the extremal values of the functions on the right of equation (60) and the remarks which follow equation (55) it is found that

$$\rho_o = \begin{cases} 3 & \text{if } \mu > \frac{1}{3}, \\ \frac{1}{\mu} & \text{if } \mu < \frac{1}{3}. \end{cases} \tag{62}$$

Now the general optimum fibre-density for uniaxial tension applied in a predetermined direction is

$$\rho_o = 1, \tag{63}$$

from equation (20); thus, carrying uniaxial tension in any direction requires three times the fibre needed to carry the same unidirectional tension. Equation (63) also represents the minimum density of solid sheet needed for arbitrarily directed uniaxial tension. For this applied load, optimum reinforced sheet is thus one third as efficient as the corresponding solid sheet; the cautionary remarks of Section 3.3, on making such a direct comparison, apply here also.

The above comparison also holds for sheets having more than three fibre directions. From Cox's analysis[1] for sheets reinforced in a number of different directions it may be shown that the optimum density of any sheet equally reinforced at equiangular intervals and subjected to arbitrarily directed uniaxial tension is also given by equation (62); the result is thus also true for the random fibre mat, which may be regarded as the limiting case of such fibre-arrangements.

7 LOAD ENVELOPES OF OPTIMUM SYSTEMS

While any structure may be optimised with regard to applied loads within a specified envelope, in practice it may occasionally also be subjected to loads which lie outside this envelope. The ability to resist such unexpected loads could well be a factor in considering the practicability of an optimum system; in particular, if other near-optimum systems existed, the ability to carry particular types of load outside the design envelope could well be a crucial point of comparison. For example, in the fibre-systems of Sections 3 and 5 the specified applied load involves only longitudinal tension

combined with shear. The ability of the optimum systems to resist transverse load is clearly of interest as, also, is the ability of the systems to resist occasional excesses of the design loads beyond their specified values. The total load-envelopes of the optimum arrangements of Sections 3-5 are therefore considered. These fibre-arrangements are of interest in this respect. They include two examples, one symmetric and one asymmetric, optimised with respect to two applied loads only in which the variation of the third load appears via the optimum solution, while the other example is of a system optimised with respect to all three applied loads.

In Sections 3 to 5 attention was focused on the l.s. and t.s. reinforcement systems. The fibre forces in the l.s. system are given by equation (6) and, since the fibre-forces (P,Q,R) are all restricted by the inequality (14), the following hold:

$$\left.\begin{aligned} -\mu\, p\, U < \tfrac{1}{2} T_2 \operatorname{cosec}^2\alpha + S \operatorname{cosec} 2\alpha < p\, U, \\ -\mu\, p\, U < \tfrac{1}{2} T_2 \operatorname{cosec}^2\alpha - S \operatorname{cosec} 2\alpha < p\, U, \\ -\mu\, r\, U < T_1 - T_2 \cot^2\alpha < r\, U. \end{aligned}\right\} \qquad (64)$$

These defined the bounding envelope in three-dimensional load-space (T_1, T_2, S); this region is the interior of a hexahedral prism whose faces are the planes

$$\left.\begin{aligned} \tfrac{1}{2} T_2 \operatorname{cosec}^2\alpha + S \operatorname{cosec} 2\alpha &= p\, U, \\ \tfrac{1}{2} T_2 \operatorname{cosec}^2\alpha + S \operatorname{cosec} 2\alpha &= -\mu\, p\, U, \\ \tfrac{1}{2} T_2 \operatorname{cosec}^2\alpha - S \operatorname{cosec} 2\alpha &= p\, U, \\ \tfrac{1}{2} T_2 \operatorname{cosec}^2\alpha - S \operatorname{cosec} 2\alpha &= -\mu\, p\, U, \end{aligned}\right\} \quad (a)$$

$$\left.\begin{aligned} T_1 - T_2 \cot^2\alpha &= r\, U, \\ T_1 - T_2 \cot^2\alpha &= -\mu\, r\, U. \end{aligned}\right\} \quad (b) \qquad (65)$$

The four planes of equation (65a) are parallel in pairs, parallel to the T_1-axis and bound an infinite prism whose cross-section is a rhombus of vertex angle α; the interior of the hexahedron is the section of this prism lying between the two parallel planes of equation (65b) (which are themselves parallel

to the S-axis). This bounding surface is shown schematically in Fig.19; since this figure illustrates further points which will be made in Sections 7.1, 7.2 and 7.4, the prism cross-section is shown to be square.

The load-envelope of the t.s. system is similar to that of the l.s. system, except that the roles of T_1 and T_2 are interchanged. With this qualification, the foregoing remarks apply; such a load-envelope is shown schematically in Fig.20, which also illustrates points to be made in Sections 7.1 and 7.4.

The load-envelope of a sheet of generally oriented fibres will follow, in the above manner, from equations (3) and (14). This will also be a hexadron in (T_1, T_2, S) space, having three pairs of parallel faces.

7.1 *Uniaxial tension and symmetric variation of shear*

The arrangement first considered is the l.s. system given by equation (20). The faces of the load-envelope are the planes

$$\left.\begin{aligned} T_2 + S &= -\lambda T, \quad T_2 + S = \frac{\lambda}{\mu} T, \\ T_2 - S &= -\lambda T, \quad T_2 - S = \frac{\lambda}{\mu} T, \end{aligned}\right\} \text{ (a)}$$

$$T_2 - T_1 = -T, \quad T_2 - T_1 = \mu T, \qquad \text{(b)} \tag{66}$$

from equations (20) and (65). These planes bound a hexahedral prism of square cross-section, which is illustrated in Fig.19; the area represented by the applied load system of equation (18) is indicated by the intersection of this surface with the (T_1, S) plane.

The complete intersection of the bounding region with the (T_1, S) plane is also of interest, being related to the allowable envelope of loads for which the system was optimised. This intersection is

$$\left.\begin{aligned} -\mu T < T_1 < T, \\ T_2 = 0, \\ -\lambda T < S < \lambda T, \end{aligned}\right\} \tag{67}$$

from equation (66); in addition to the applied load of equation (18), combined uniaxial compression and shear in the range

$$\left.\begin{aligned} -\mu T < T_1 &< 0, \\ -\lambda T < S &< \lambda T \end{aligned}\right\}$$

can also be carried.

Also of interest is the shape of the bounding region near the (T_1, S) plane, since this gives possible small variations of the transverse load T_2 not allowed for in the optimisation. It can be shown that the region

$$\left.\begin{aligned} 0 < T_1 &< T, \\ -\lambda T < S &< \lambda T, \\ 0 < T_2 &< \begin{cases} \dfrac{\lambda}{\mu}(1-\mu)\,T & \text{if } \lambda < \dfrac{\mu^2}{1-\mu}, \\ \mu T & \text{if } \lambda > \dfrac{\mu^2}{1-\mu} \end{cases} \end{aligned}\right\} \qquad (68)$$

lies wholly within the bounding surface; this is also illustrated in Fig.19. Some unrestricted tensile variation of T_2 is thus permissible; further tensile and compressive variation of T_2 are possible, but both are governed by the shape of the load envelope and, as may readily be seen from Fig.19, can only take place if corresponding restrictions are placed on T_1 and S.

The above l.s. fibre system was shown in Section 3.1 to be the general optimum for uniaxial applied tension and symmetric shear; however for the particular shear given by equation (29) the t.s. arrangement gave rise to the same fibre density, while other fibre arrangements with densities close to the optimum existed in this vicinity. The load envelope of this t.s. system is therefore considered; this is the hexahedral rhombic prism which is bounded by the planes

$$\left.\begin{aligned} T_1 + \frac{S}{\mu} &= \frac{T}{1-\mu}, \quad T_1 + \frac{S}{\mu} = -\frac{\mu T}{1-\mu}, \\ T_1 - \frac{S}{\mu} &= \frac{T}{1-\mu}, \quad T_1 - \frac{S}{\mu} = -\frac{\mu T}{1-\mu}, \\ -\mu T_1 + \frac{1}{\mu} T_2 &= T, \quad -\mu T_1 + \frac{1}{\mu} T_2 = -\mu T, \end{aligned}\right\} \qquad (69)$$

from equations (7), (14) and (29). This region is shown schematically in Fig.20; the area represented by the applied load of equation (18) is indicated.

The intersection of the bounding region of equation (69) with the (T_1, S) plane determines the allowable envelope of forces for which the system was optimised; this region,

$$\left.\begin{aligned} -\frac{\mu}{1-\mu} T < T_1 + \frac{1}{\mu} S < \frac{1}{1-\mu} T, \\ -\frac{\mu}{1-\mu} T < T_1 - \frac{1}{\mu} S < \frac{1}{1-\mu} T, \\ -\frac{T}{\mu} < T_1 < T, \end{aligned}\right\}$$

is shown in Fig.21 where it is compared with the corresponding region for the l.s. arrangement (cf. equation (67)) when $\mu = 0{\cdot}6$. The optimum l.s. system allows for the additional development of compressive T_1 in the range

$$-\mu T < T_1 < 0$$

in conjunction with the full range of shear. The t.s. system allows small increases in shear for tensile T_1 which is less than the maximum value T, while compressive T_1 is possible only if the shear is restricted. These points typify the considerations which might arise if deciding between competing optimum and near-optimum systems.

Permissible variations of T_2 are governed by the inequalities

$$\left.\begin{aligned} 0 < T_1 < T, \\ -\lambda T < S < \lambda T, \\ 0 < T_2 < \mu T, \end{aligned}\right\}$$

which define a region lying inside the bounding surface; this is also shown in Fig.20. Small tensile variations of T_2 are thus again unconditionally possible in combination with the full variation in T_1 and S; tensile and compressive T_2 variations beyond these limits are governed by the shape of the bounding surface, and can only take place if T_1 and S are restricted. It is of interest that both the l.s. and t.s. system allow additional variations in the transverse load T_2; since the l.s. system is the general optimum while the t.s. system corresponds only to a particular value of the shear, they do not compete directly however.

7.2 Biaxial tension and symmetric variation of shear

It was shown in Section 4.1 that in all cases the l.s. distribution was the optimum; the load envelope is therefore that bounded by the planes of equation (65) and illustrated schematically in Fig.19. For increasing λ the actual shape of the load envelope will vary, since it depends for its detailed form on the fibre-distribution defined by equations (38) and (39). For $0{\cdot}5 < \mu < 1$ and large values of the shear the optimum distribution is that of equation (39c), and this is the same as that derived for the load system of uniaxial tension and combined shear in Section 3.1. The analysis of Section 7.1 relevant to the l.s. fibre-distribution therefore applies here also; in particular, the rectangular solid shown in Fig.19 now corresponds to the applied load envelope of equation (33).

7.3 Uniaxial tension and asymmetric variation of shear

In the optimised arrangements in which the shear is allowed to vary between asymmetric limits, the fibre orientations and densities are given by equation (54). If this optimum system is subjected to a general applied load, the fibre forces are given by

$$\left.\begin{aligned} p_o P &= T_2 + S \cot \alpha_o, \\ q_o Q &= T_2 - S \tan \alpha_o, \\ r_o R &= T_1 - T_2 - 2S \cot 2\alpha_o, \end{aligned}\right\} \qquad (70)$$

from equation (3). The load envelope is thus the hexadron cut from the infinite rectangular prism bounded by the planes

$$\left.\begin{aligned} T_2 \tan \alpha_o + S &= -\lambda \mu T, \quad T_2 \tan \alpha_o + S = \lambda T, \\ T_2 \cot \alpha_o - S &= -\lambda T, \quad T_2 \cot \alpha_o - S = \frac{\lambda}{\mu} T, \end{aligned}\right\} \qquad (71a)$$

which are parallel to the T_1-axis, by the two parallel planes

$$T_1 - T_2 - 2S \cot 2\alpha_o = -\mu T, \quad T_1 - T_2 - 2S \cot 2\alpha_o = T. \qquad (71b)$$

This region is shown schematically in Fig.22 for small values of the shear corresponding to equation (54b); the relation to the bounding surface of the area represented by the applied load of equation (48) is indicated. In

contrast to the system of Section 7.1, tensile and compressive variations of T_2 near the region of equation (48), for which the optimisation was carried out, can only take place if T_1 and S are correspondingly restricted.

The intersection of the load-envelope with the (T_1, S) plane is shown in Fig.23, for $\mu = 0{\cdot}6$ and small values of the shear (cf. equation (54b)); to illustrate allowable 'unexpected' load variations, the area corresponding to equation (48) is also indicated. Negative values of the shear S can only be allowed if restrictions on T_1 are introduced. Compressive T_1 variation in the range

$$-\frac{T}{\sqrt{\mu}}\{\mu\sqrt{\mu} - \lambda(1-\mu)\} < T_1 < 0 \qquad (72)$$

is allowable without any corresponding restriction on the shear; this no longer holds, however, for larger limits of shear which correspond to equation (54a), and compressive T_1 variation then also implies restrictions on S.

7.4 Isotropic arrangements

The symmetric isotropic arrangements which have been considered will have similar load-envelopes to those discussed in Section 7.1; the envelope will be a hexahedral prism of 120° rhombic cross-section whose faces will be defined as in equation (65) for l.s. systems. Figs.19 and 20 thus serve to give a schematic indication of the load-envelope in this case also.

8 CONCLUDING REMARKS

A technique has been presented for the optimisation of the fibre systems in reinforced sheets having three directions of reinforcement and subjected to combined tensile and shearing load systems. The theory is based on the conventional assumption of netting analysis that the load is carried axially in the fibres. All the systems which are found to be optimum for the load-envelopes considered have one set of fibres aligned in the direction in which the tension is allowed the larger variation. In cases involving uniaxial tension the quantities of those fibres which carry shear are determined entirely by the magnitude of the shear while for asymmetric shear variations these fibres are best aligned asymmetrically; the tension-carrying fibres are also determined entirely by the tension in this case.

Two assessments of the efficiency of reinforced sheet are made. To assess fibre-reinforcement solely as a mode of construction the optimum fibre

densities are compared with those of solid sheet made of material having the fibre properties. For the systems of combined tension and shear the lowest fibre-efficiency (regarded as a density-ratio) is found to be 0·43 when there is no fall-off in compressive fibre performance and is 0·20 if considerable fall-off is assumed. If arbitrarily directed uniaxial tension is considered and there is no fall-off in compressive fibre performance the efficiency is 0·33. All these figures will be further reduced in an actual composite by fibre-inefficiency and the presence of a matrix.

To assess the practicability of such standard forms of composite construction as isotropic sheet the second comparison made is between optimum and isotropic systems of reinforcement. It is found that, given reasonable fibre compressive properties, the density of optimum sheet lies between 0·5 and 0·99 of the density of the best-orientated isotropic sheet. In particular cases, at intermediate values of the shear, isotropic sheet shows up favourably since the amount of shear happens to 'fit' the isotropic alignment.

The total allowable load-envelopes of both optimum and near-optimum configurations are also considered and provide criteria of choice in any particular application. It is known[5], for example, that structures optimised for one given load condition can exhibit unwelcome properties in other load conditions; no such behaviour is observed in the present Paper.

Appendix A

ELASTIC CONSTANTS OF REINFORCED SHEETS

(see Section 2)

This Paper has derived optimum distributions of fibre for particular load-envelopes; for completeness, this Appendix gives expressions for the elastic constants of the optimum systems which have been found. The analysis follows that of Cox[1].

In an aeolotropic sheet in which the strains are $(\varepsilon_x, \varepsilon_y, \gamma_{xy})$ the loads carried in typical (P,Q,R)-fibres are

$$\left.\begin{aligned} P &= A E (\varepsilon_x \cos^2 \alpha + \varepsilon_y \sin^2 \alpha + \gamma_{xy} \sin \alpha \cos \alpha), \\ Q &= A E (\varepsilon_x \cos^2 \beta + \varepsilon_y \sin^2 \beta + \gamma_{xy} \sin \beta \cos \beta), \\ R &= A E (\varepsilon_x \cos^2 \gamma + \varepsilon_y \sin^2 \gamma + \gamma_{xy} \sin \gamma \cos \gamma), \end{aligned}\right\} \quad (73)$$

where E is the stiffness of the fibre material. If the stresses are based on the effective sheet thickness (i.e. the volume of fibre per unit area of sheet) so that

$$(\sigma_x, \sigma_y, \tau_{xy}) = \frac{U}{\rho A T} (N_x, N_y, N_{xy}), \quad (74)$$

then the stress-strain relations are

$$\left.\begin{aligned} \sigma_x &= c_{11} \varepsilon_x + c_{12} \varepsilon_y + c_{16} \gamma_{xy}, \\ \sigma_y &= c_{12} \varepsilon_x + c_{22} \varepsilon_y + c_{26} \gamma_{xy}, \\ \tau_{xy} &= c_{16} \varepsilon_x + c_{26} \varepsilon_y + c_{12} \gamma_{xy}, \end{aligned}\right\} \quad (75)$$

from equations (1), (2), (73) and (74), where the elastic constants are given by

$$\left.\begin{aligned} \frac{\rho T}{E U} c_{11} &= p \cos^4 \alpha + q \cos^4 \beta + r \cos^4 \gamma, \\ \frac{\rho T}{E U} c_{12} &= p \sin^2 \alpha \cos^2 \alpha + q \sin^2 \beta \cos^2 \beta + r \sin^2 \gamma \cos^2 \gamma, \\ \frac{\rho T}{E U} c_{22} &= p \sin^4 \alpha + q \sin^4 \beta + r \sin^4 \gamma, \\ \frac{\rho T}{E U} c_{16} &= p \sin \alpha \cos^3 \alpha + q \sin \beta \cos^3 \beta + r \sin \gamma \cos^3 \gamma, \\ \frac{\rho T}{E U} c_{26} &= p \sin^3 \alpha \cos \alpha + q \sin^3 \beta \cos \beta + r \sin^3 \gamma \cos \gamma. \end{aligned}\right\} \quad \ldots\ (76)$$

Note that

$$c_{11} + 2c_{12} + c_{22} = E.$$

A.1 Longitudinally symmetric arrangements

For a general l.s. system

$$\left.\begin{aligned} \frac{\rho T}{E U} c_{11} &= 2p \cos^4 \alpha + r, \quad \frac{\rho T}{E U} c_{12} = 2p \sin^2 \alpha \cos^2 \alpha, \\ \frac{\rho T}{E U} c_{22} &= 2p \sin^4 \alpha, \quad c_{16} = c_{26} = 0, \end{aligned}\right\} \quad (77)$$

from equations (4) and (76); this system is orthotropic. In Sections 3.1 and 4.1 the particular l.s. system of equation (20) was found to be the optimum, and in this case the elastic constants are

$$c_{11} = \frac{(\lambda + 2\mu) E}{2(2\lambda + \mu)}, \quad c_{12} = c_{22} = \frac{\lambda E}{2(2\lambda + \mu)}, \quad c_{16} = c_{26} = 0. \quad \ldots\ (78)$$

A.2 Transversely symmetric arrangements

For a general t.s. system,

$$\left.\begin{aligned} \frac{\rho T}{E U} c_{11} &= 2p \cos^4 \alpha, \quad \frac{\rho T}{E U} c_{12} = 2p \sin^2 \alpha \cos^2 \alpha, \\ \frac{\rho T}{E U} c_{22} &= 2p \sin^4 \alpha + q, \quad c_{16} = c_{26} = 0, \end{aligned}\right\} \quad (79)$$

from equations (5) and (76); this system is also orthotropic. For the particular t.s. system which was found to be optimum in Sections 3.1 and 4.1, the elastic constants are

$$\left.\begin{aligned} c_{11} &= \frac{E}{(1 + \mu)(1 + \mu^2)}, \quad c_{12} = \mu^2 c_{11}, \\ c_{22} &= \mu(1 - \mu + \mu^2) c_{11}, \quad c_{16} = c_{26} = 0, \end{aligned}\right\} \quad (80)$$

from equations (27d), (29) and (79).

A.3 Isotropic arrangements

The general isotropic arrangement is that defined by equation (8); in this case

$$c_{11} = c_{22} = 3E/8, \quad c_{12} = E/8, \quad c_{16} = c_{26} = 0, \tag{81}$$

from equation (76). The elastic properties of the sheet are thus those of an isotropic elastic sheet having a Young's modulus of $3E/8$, a shear modulus of $E/8$ and a Poisson's ratio of $1/3$.

A.4 Asymmetric optimum arrangement

The elastic constants of the asymmetric system of Section 4.1 may also be derived; they are given by

$$\left.\begin{aligned}
\frac{\mu \rho_o}{\lambda E} c_{12} &= \sin \alpha_o \cos \alpha_o (\sin^2 \alpha_o + \mu \cos^2 \alpha_o), \\
\frac{\mu \rho_o}{\lambda E} c_{22} &= \sin \alpha_o \cos \alpha_o (\mu \sin^2 \alpha_o + \cos^2 \alpha_o), \\
c_{11} &= E - c_{22} - 2c_{12}, \\
\frac{\mu \rho_o}{\lambda E} c_{16} &= \mu \cos^4 \alpha_o - \sin^4 \alpha_o, \\
\frac{\mu \rho_o}{\lambda E} c_{26} &= -(1 - \mu) \sin^2 \alpha_o \cos^2 \alpha_o,
\end{aligned}\right\} \tag{82}$$

from equations (54) and (76); this system is aeolotropic but, since the right-hand sides of equations (82) depend on two parameters (λ; μ) only, relationships exist between the elastic constants.

Appendix B

FIBRE DENSITY FOR SYSTEMS SUBJECTED TO UNIAXIAL TENSION WITH ASYMMETRICALLY VARYING SHEAR

(see Section 5.1)

Under the asymmetric applied load of equation (48), the fibre-forces P, Q and R are given by equation (49). It will be necessary to consider the form taken by the fibre density when the condition $180° \geq \gamma > \beta > \alpha > 0$ is relaxed and it is merely assumed that $\gamma > \beta > \alpha$, $\gamma - \beta < 180°$ and $\beta - \alpha < 180°$. In this case the densities p, q and r take different forms depending on a number of inequalities. The following expressions are derived for the minimum values of p, q and r, the densities being determined to be just sufficient to carry the loads of equation (48);

$$\frac{U}{T}\, p \sin(\gamma-\alpha) \sin(\beta-\alpha) =$$

$$\begin{cases} \max\left\{\sin\gamma \sin\beta, \frac{\lambda}{\mu}\sin(\gamma+\beta)\right\} & \text{if } \sin(\gamma+\beta)>0,\ \sin\gamma\sin\beta>0, \quad (a) \\ \frac{\lambda}{\mu}\sin(\gamma+\beta) - \frac{1}{\mu}\sin\gamma\sin\beta & \text{if } \sin(\gamma+\beta)>0,\ \sin\gamma\sin\beta<0, \quad (b) \\ \sin\gamma\sin\beta - \lambda\sin(\gamma+\beta) & \text{if } \sin(\gamma+\beta)<0,\ \sin\gamma\sin\beta>0, \quad (c) \\ \max\left\{-\lambda\sin(\gamma+\beta), -\frac{1}{\mu}\sin\gamma\sin\beta\right\} & \text{if } \sin(\gamma+\beta)<0,\ \sin\gamma\sin\beta<0, \quad (d) \end{cases}$$

.... (83)

corresponding to limiting tensile and compressive P for points on the load envelope,

$$\frac{U}{T}\, q \sin(\gamma-\beta) \sin(\beta-\alpha) =$$

$$\begin{cases} \max\left\{\lambda\sin(\alpha+\gamma), \frac{1}{\mu}\sin\alpha\sin\gamma\right\} & \text{if } \sin(\alpha+\gamma)>0,\ \sin\alpha\sin\gamma>0, \quad (a) \\ -\sin\gamma\sin\alpha + \lambda\sin(\alpha+\gamma) & \text{if } \sin(\alpha+\gamma)>0,\ \sin\alpha\sin\gamma<0, \quad (b) \\ \frac{1}{\mu}\sin\alpha\sin\gamma - \frac{\lambda}{\mu}\sin(\alpha+\gamma) & \text{if } \sin(\alpha+\gamma)<0,\ \sin\alpha\sin\gamma>0, \quad (c) \\ \max\left\{-\sin\alpha\sin\gamma, -\frac{\lambda}{\mu}\sin(\alpha+\gamma)\right\} & \text{if } \sin(\alpha+\gamma)<0,\ \sin\alpha\sin\gamma<0, \quad (d) \end{cases}$$

.... (84)

corresponding to limiting Q for points on the load envelope, and

$$\frac{U}{T} r \sin(\gamma-\beta) \sin(\gamma-\alpha) =$$

$$\begin{cases} \max\left\{\sin\alpha \sin\beta, \frac{\lambda}{\mu}\sin(\alpha+\beta)\right\} & \text{if } \sin(\alpha+\beta)>0,\ \sin\alpha\sin\beta>0, \quad (a) \\ -\frac{1}{\mu}\sin\alpha\sin\beta + \frac{\lambda}{\mu}\sin(\alpha+\beta) & \text{if } \sin(\alpha+\beta)>0,\ \sin\alpha\sin\beta<0, \quad (b) \\ \sin\alpha\sin\beta - \lambda\sin(\alpha+\beta) & \text{if } \sin(\alpha+\beta)<0,\ \sin\alpha\sin\beta>0, \quad (c) \\ \max\left\{-\lambda\sin(\alpha+\beta), -\frac{1}{\mu}\sin\alpha\sin\beta\right\} & \text{if } \sin(\alpha+\beta)<0,\ \sin\alpha\sin\beta<0, \quad (d) \end{cases} \quad \ldots. (85)$$

corresponding to limiting R. The density is obtained by adding the values of p, q and r given by equations (83) to (85). If the assumption is made that $\gamma = 180°$, equation (50) is recovered; it has been shown in Section 5.1, that a minimum of the density for variations in α and β only is found in equation (50) when

$$\gamma = 180°, \quad \beta_o = 90° + \alpha_o \qquad (54a)\text{ bis}$$

and α_o is given by equations (54b, c). If small variations in γ from the above are taken and

$$\gamma = 180° - \delta, \qquad (86)$$

where δ is small, then the densities p, q and r are given from equations (83) to (85) to be:

$$\frac{U}{T} p \sin(\gamma-\alpha_o) = \begin{cases} \sin\gamma\sin\beta_o - \lambda\sin(\gamma+\beta_o) & \text{if } \delta>0, \\ -\lambda\sin(\gamma+\beta_o) & \text{if } \delta<0, \end{cases} \quad \ldots. (87)$$

$$\frac{U}{T} q \sin(\gamma-\beta_o) = \begin{cases} \frac{1}{\mu}\sin\alpha_o\sin\gamma - \frac{\lambda}{\mu}\sin(\alpha_o+\gamma) & \text{if } \delta>0, \\ -\frac{\lambda}{\mu}\sin(\alpha_o+\gamma) & \text{if } \delta<0, \end{cases} \quad \ldots. (88)$$

and

$$\frac{U}{T} r \sin(\gamma - \beta_o) \sin(\gamma - \alpha_o) = \sin \alpha_o \sin \beta_o ; \qquad (89)$$

in deriving equations (87) to (89), use has been made of the fact that $\sin(\gamma + \beta_o) < 0$, $\sin(\gamma + \alpha_o) < 0$, $\sin(\alpha_o + \beta_o) > 0$ (cf. the remarks following equation (50)), $\sin(\beta_o - \alpha_o) = 1$ (from equation (54a)) and the fact that $\sin \gamma$ is small.

For small δ, each of p, q and r can be derived to the first order in δ from equations (87) to (89); the density ρ follows and, to the first order,

$$\rho - \rho_o = \left\{ \begin{array}{ll} \delta \left\{ \frac{1-\mu}{\sqrt{\mu}} + 2\frac{1-\mu}{\mu}\left(\frac{\mu\sqrt{\mu}}{1-\mu} - \lambda\right) \right\} & \text{if } \delta > 0 \\ -\delta(1-\mu)\left(\frac{2\lambda}{\mu} + \frac{1}{\sqrt{\mu}}\right) & \text{if } \delta < 0 \end{array} \right\} \text{ and } \lambda < \frac{\mu\sqrt{\mu}}{1-\mu} \qquad (90a)$$

and

$$\rho - \rho_o = \left\{ \begin{array}{ll} \frac{\delta}{\mu} \cot \alpha_o (\tan^2 \alpha_o - \mu^2) & \text{if } \delta > 0 \\ -\delta(1+\mu) \cot \alpha_o & \text{if } \delta < 0 \end{array} \right\} \text{ and } \lambda > \frac{\mu\sqrt{\mu}}{1-\mu} . \qquad (90b)$$

The expressions on the right-hand sides of equations (90a, b) which multiply δ (when $\delta > 0$) and $-\delta$ (when $\delta < 0$) are self-evidently positive, and so the density of the fibre system of equation (54) is a local minimum.

SYMBOLS

A zero subscript is used to denote an optimum distribution.

A	cross-sectional area of an average fibre
$c_{11}, c_{12}, c_{22}, c_{16}, c_{26}$	elastic constants of sheet
E	stiffness of fibre material
$f_1(\alpha)$, $f_2(\alpha)$	functions defined in equation (24)
$f_3(\alpha)$	function defined in equation (56b)
$g_1(\alpha)$, $g_2(\alpha)$	functions defined in equation (36a)
N_x, N_y, N_{xy}	forces in sheet
p, q, r	fibre densities per unit distance in plane of sheet
P, Q, R	tensile forces in average fibres
S	applied shear
T	typical applied tension
T_1, T_2	applied tensions in longitudinal and transverse directions
U	limiting tensile force in a single fibre; see equation (14)
α_1, α_2	particular values of α defined by equation (26)
α_1', α_2'	particular values of α defined by equation (37)
α, β, γ	fibre-orientations; see Fig.1
δ	defined by equation (86)
$\varepsilon_x, \varepsilon_y, \gamma_{xy}$	strains
θ_1, θ_2	particular values of α defined by equation (36b)
λ	ratio of limit of applied shear to limit of applied tension
λ_1, λ_2	particular values of λ defined by equation (28)
λ_3	particular value of λ defined by equation (36b)
λ_4, λ_5	particular values of λ defined by equation (40)
λ_6	particular value of λ defined as the positive root of equation (59)
$\bar{\lambda}$	see equation (52) and text preceding equation (54a)
μ	ratio of allowable compressive and tensile forces in a single fibre; see equation (14)
ρ	non-dimensional fibre density, defined by equation (15)
σ	density of fibre material
$\sigma_x, \sigma_y, \tau_{xy}$	stresses in sheet, based on effective sheet thickness
ϕ_1, ϕ_2	particular values of α defined by equations (25) and (43) respectively

REFERENCES

No.	Author	Title, etc.
1	H. L. Cox	The elasticity and strength of paper and other fibrous materials. British Journal of Applied Physics, 3, 72-79, 1952
2	H. M. Darwell G. Hughes	The application of filament winding to the manufacture of rocket motor-cases. British Plastics Federation; Proceedings of the 3rd International Reinforced Plastics Conference, Section 29, 1962
3	J. C. Schulz	Netting analysis of filament-wound pressure vessels. American Society of Mechanical Engineers, Paper No. 63-WA-223, 1963
4	P. W. Jackson D. Cratchley	The effect of fibre-orientation on the tensile strength of fibre-reinforced metals. J. Mech. Phys. Solids, 14, 49-64, 1966
5	H. L. Cox	The design of structure of least weight. Pergamon Press, 1965, Chapters 8, 9
6	L. C. Schmidt	Minimum weight layouts of elastic, statically determinate triangulated frames under alternative load systems. J. Mech. Phys. Solids, 10, 139-149, 1962
7	R. Hill	The mathematical theory of plasticity. Oxford University Press, 1950, p.300
8	M. C. Porter	The effect of filament geometry on reinforced composite strength. American Institute of Aeronautics and Astronautics, Paper No. 66-142, presented at the 3rd AIAA Aerospace Sciences Meeting, Jan. 1966
9	B. A. M. Piggott	Private communication
10	M. J. D. Powell	An efficient method for finding the minimum of a function of several variables without calculating derivatives. Computer Journal, 7, No.2, 155-162, 1964

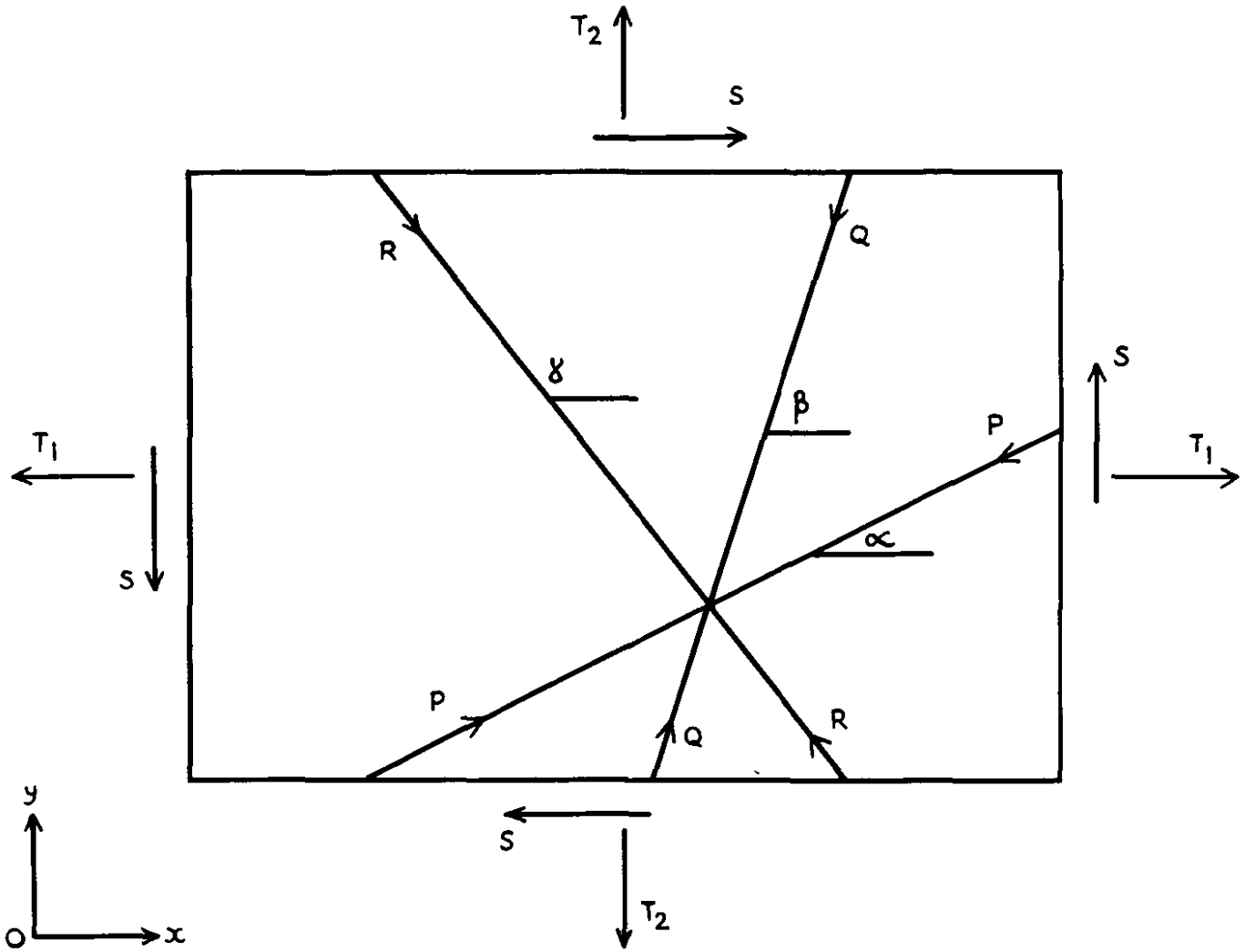

FIG. 1 FIBRE ORIENTATION AND APPLIED LOAD SYSTEM

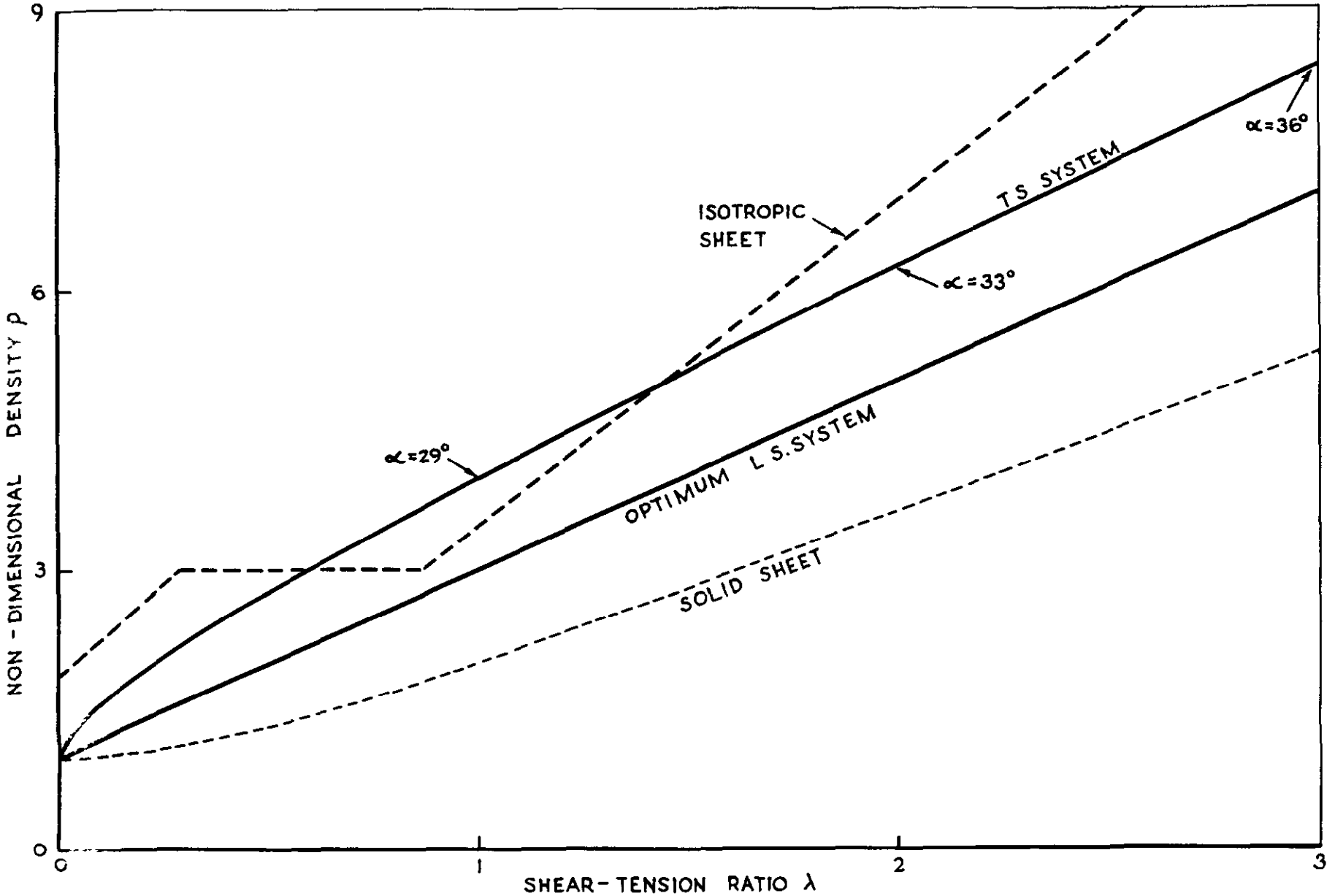

FIG.2 FIBRE DENSITIES; UNIAXIAL TENSION, SYMMETRIC SHEAR VARIATION, $\mu = 1$

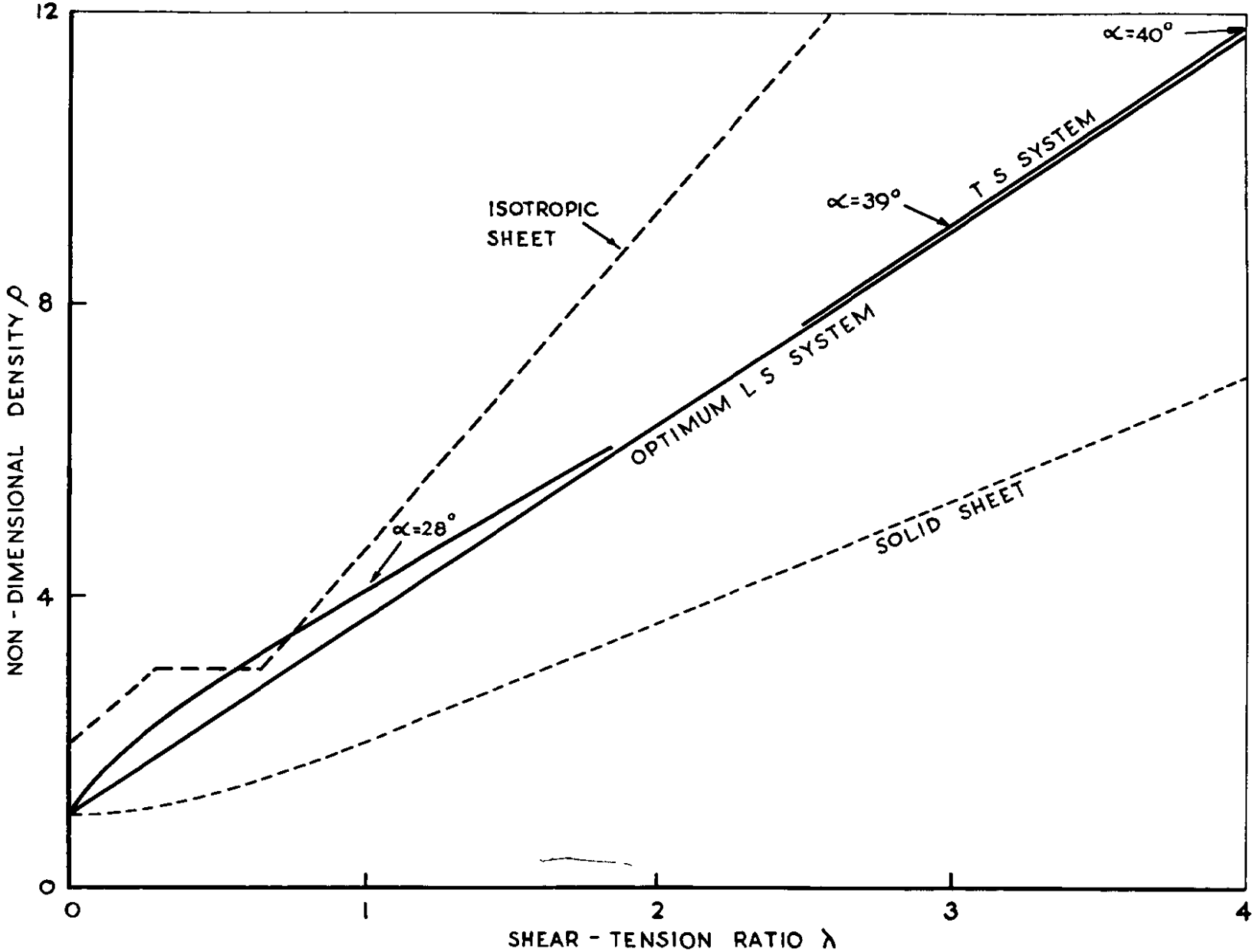

FIG 3 FIBRE DENSITIES; UNIAXIAL TENSION, SYMMETRIC SHEAR VARIATION, $\mu = 0{\cdot}75$

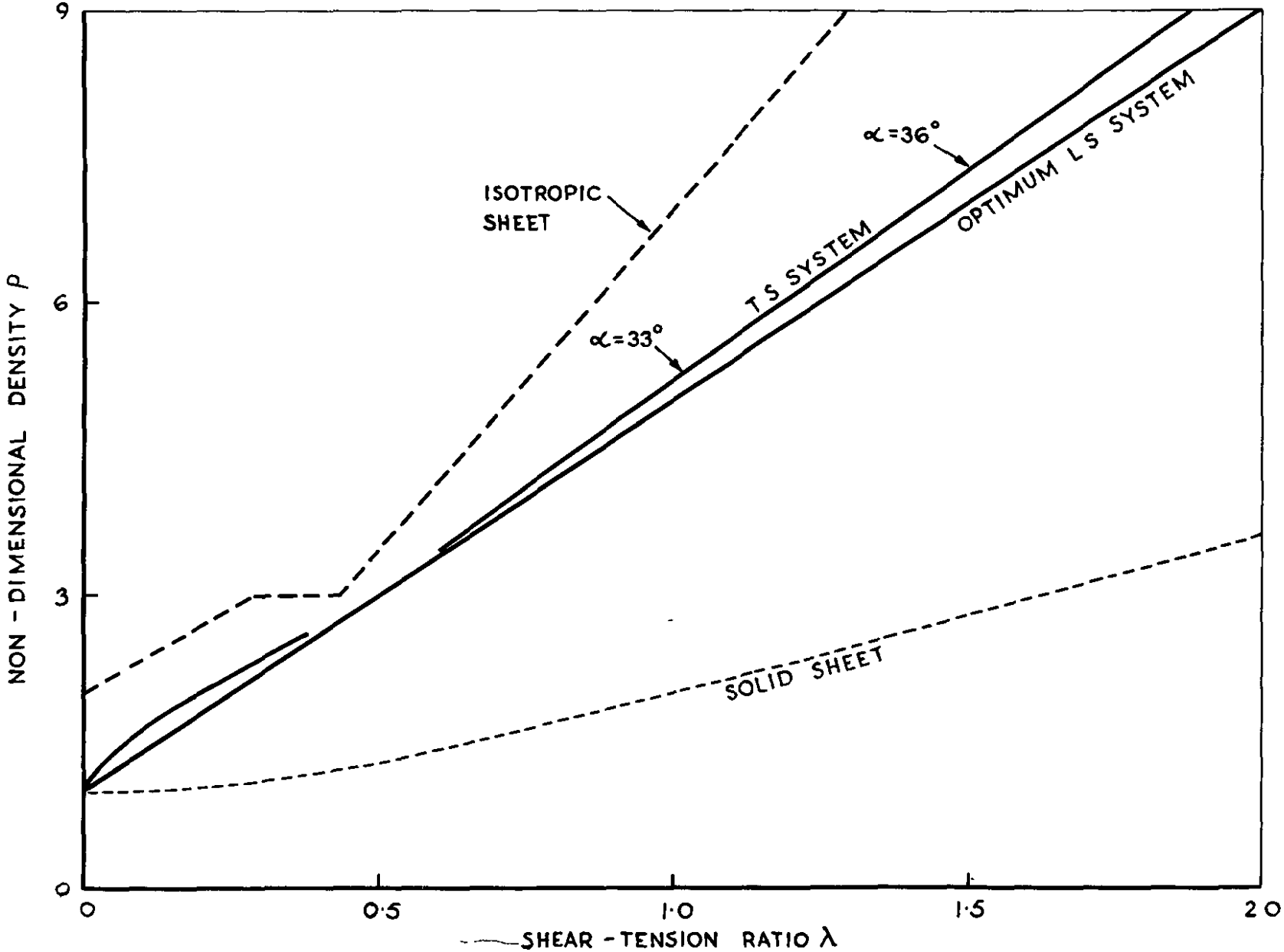

FIG.4 FIBRE DENSITIES; UNIAXIAL TENSION, SYMMETRIC SHEAR VARIATION, $\mu = 0{\cdot}5$

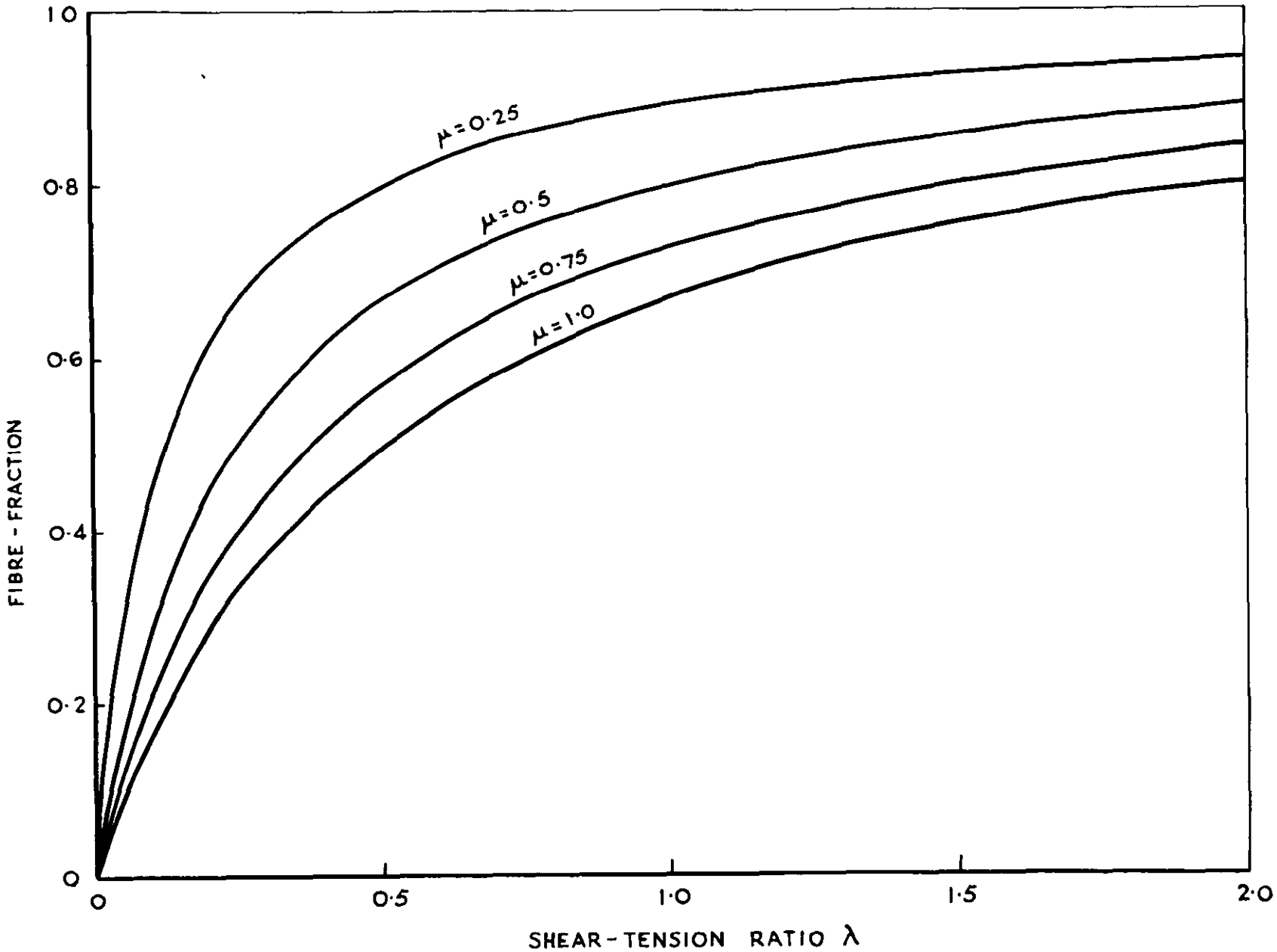

FIG.5 FIBRE FRACTION RESISTING SHEAR, UNIAXIAL TENSION, SYMMETRIC SHEAR VARIATION

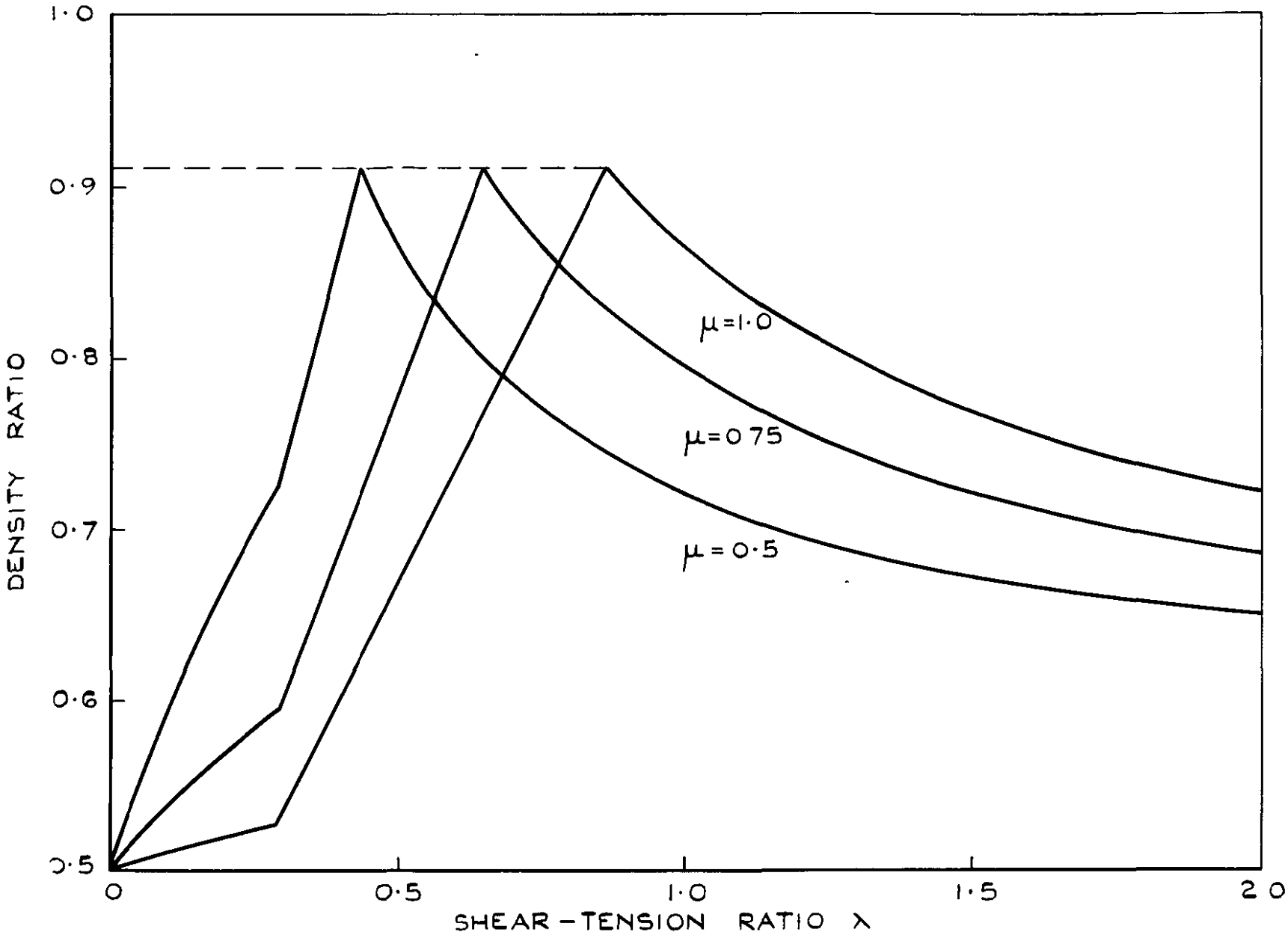

FIG 6 OPTIMUM/ISOTROPIC DENSITY RATIO; UNIAXIAL TENSION, SYMMETRIC SHEAR VARIATION

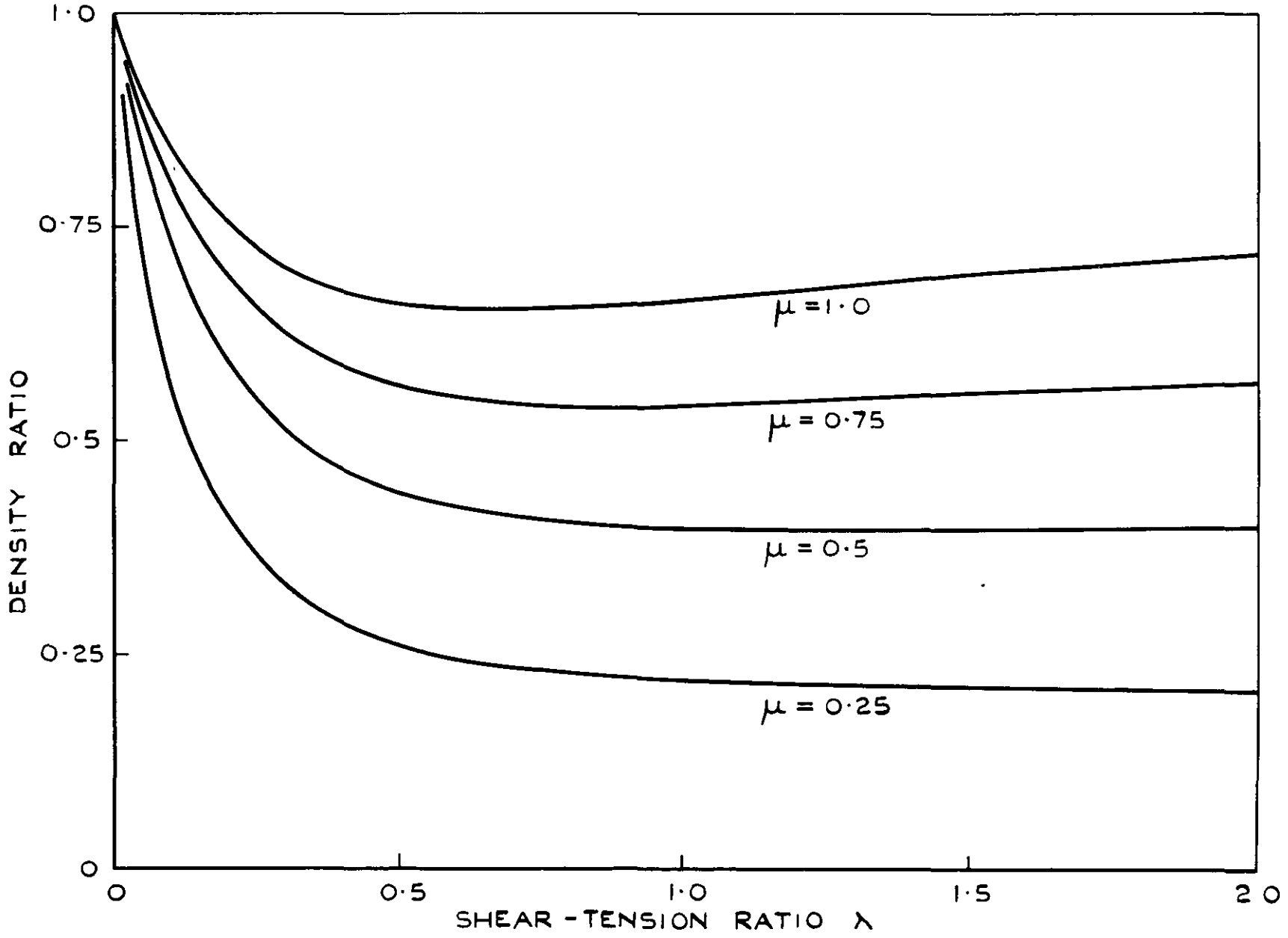

FIG 7 SOLID/OPTIMUM DENSITY RATIO; UNIAXIAL TENSION, SYMMETRIC SHEAR VARIATION

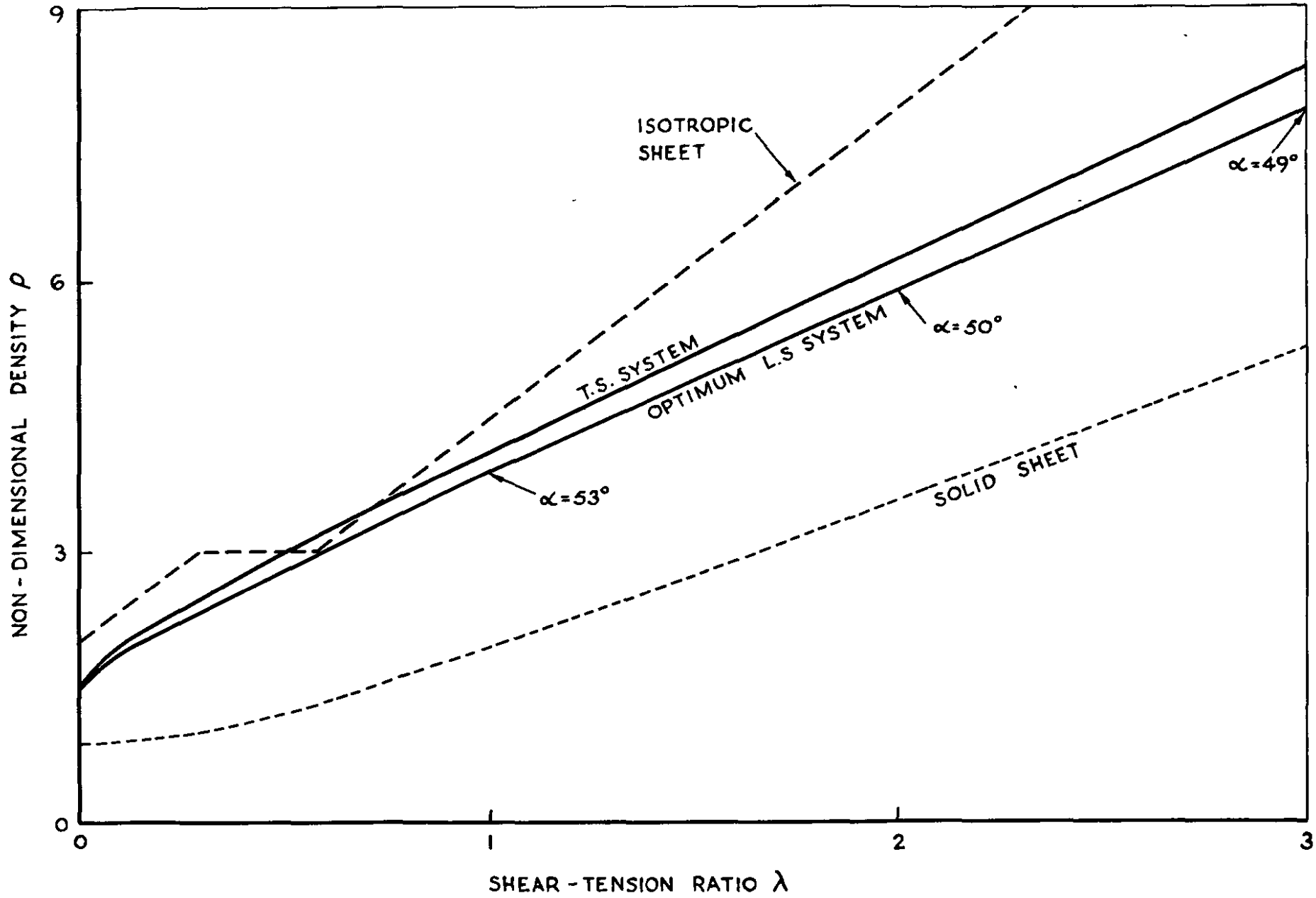

FIG. 8 FIBRE DENSITIES; BIAXIAL TENSION, SYMMETRIC SHEAR VARIATION, $\mu = 1$

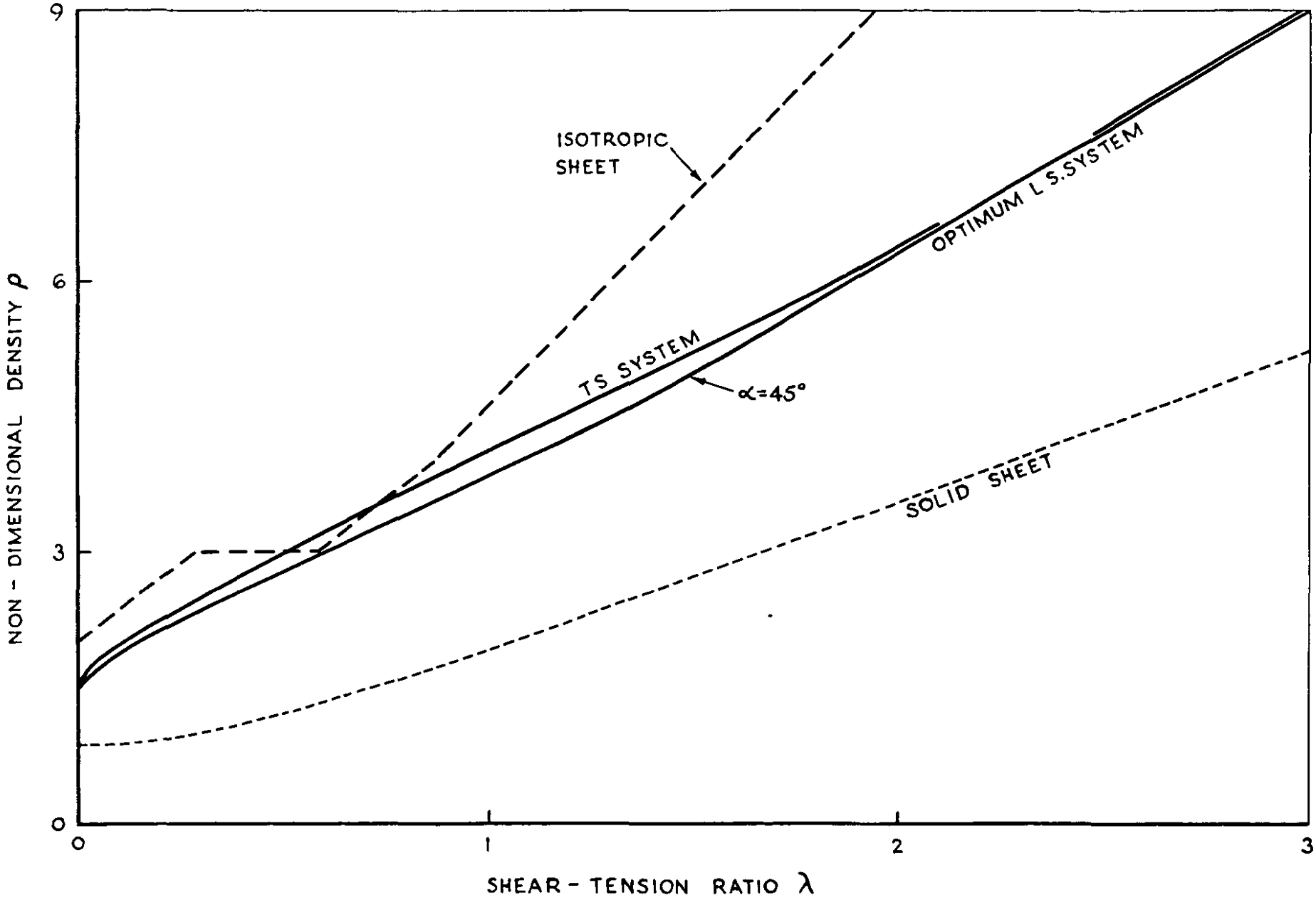

FIG 9 FIBRE DENSITIES; BIAXIAL TENSION, SYMMETRIC SHEAR VARIATION, $\mu = 0{\cdot}75$

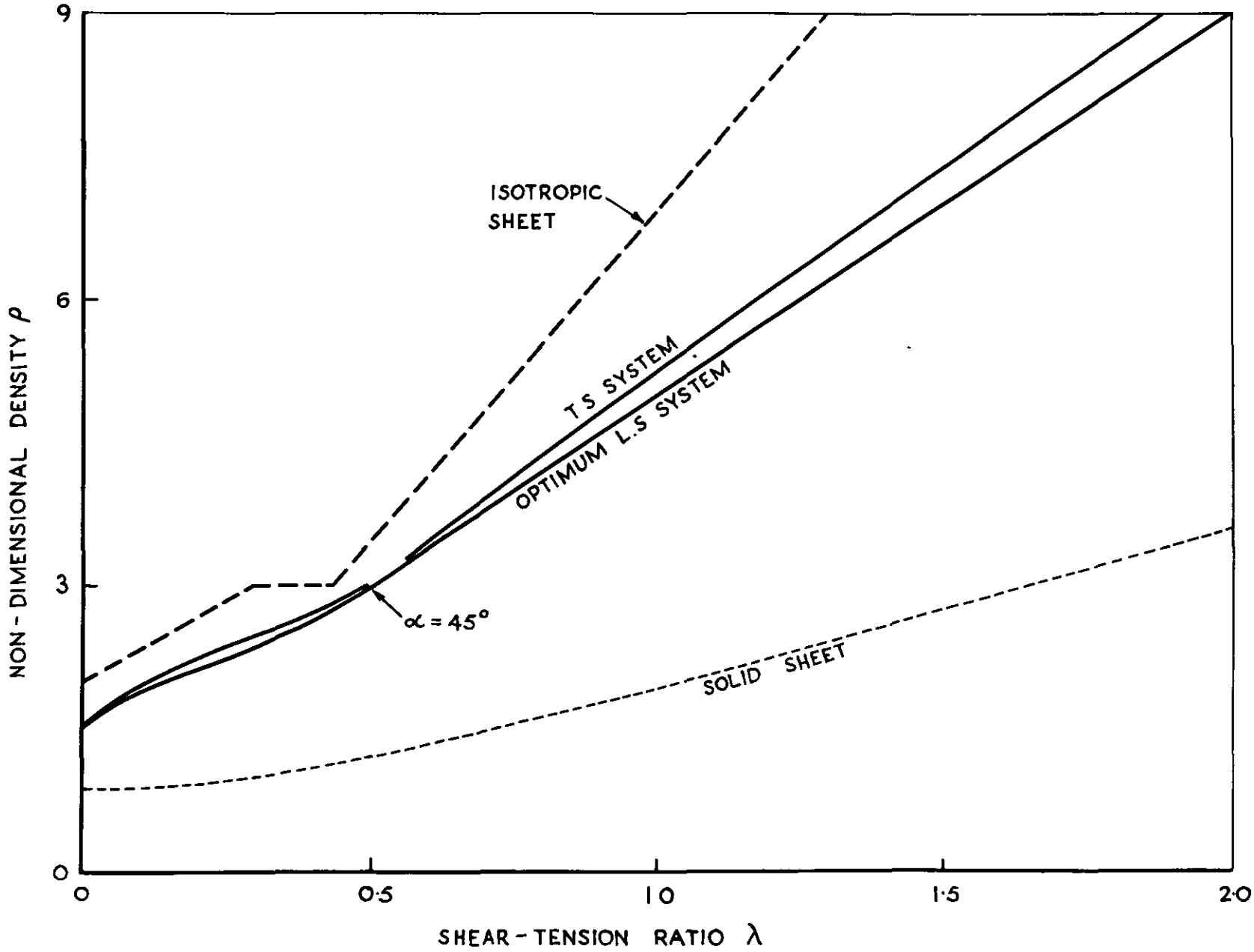

FIG.10 FIBRE DENSITIES; BIAXIAL TENSION, SYMMETRIC SHEAR VARIATION, $\mu = 0{\cdot}5$

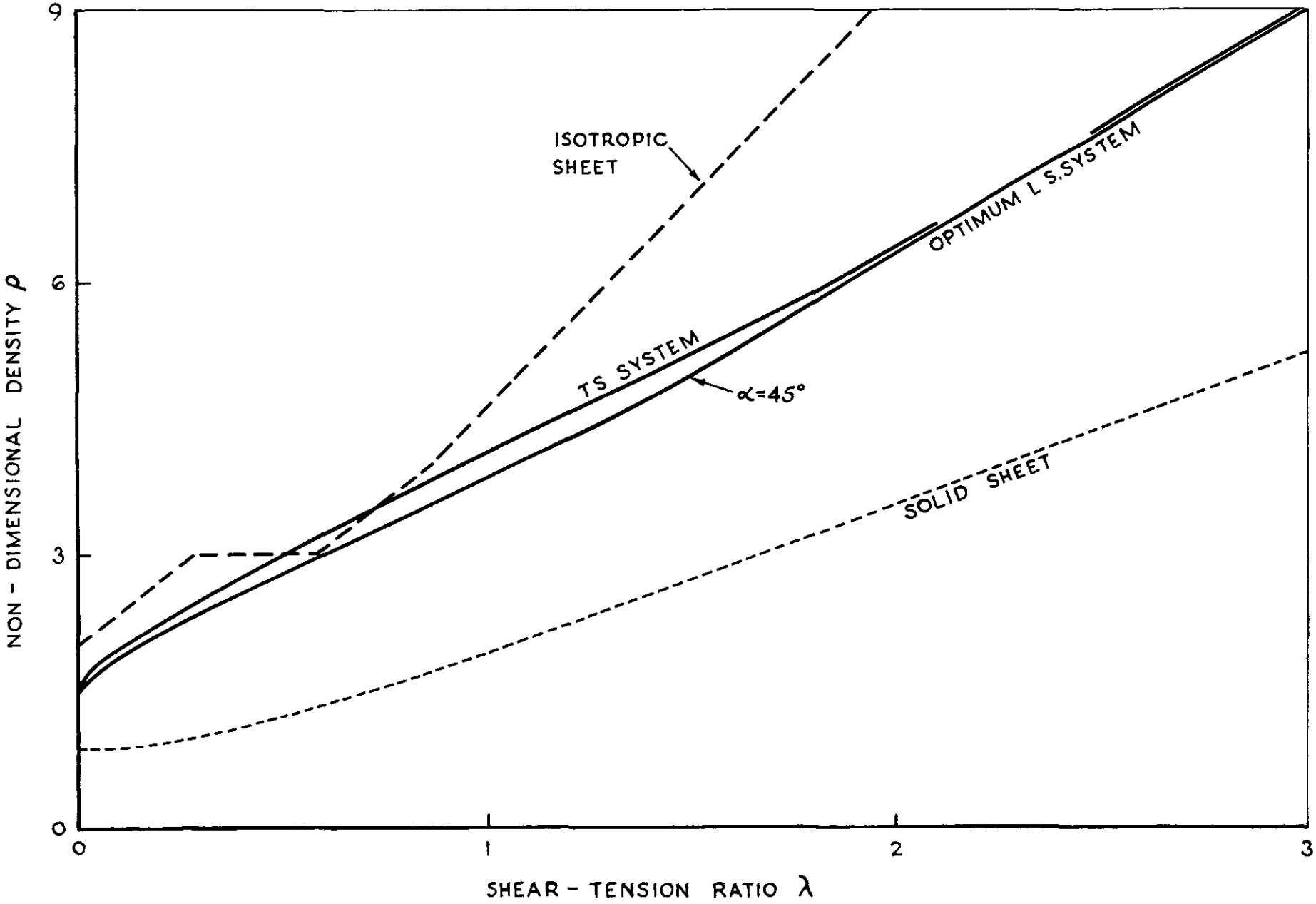

FIG 9 FIBRE DENSITIES; BIAXIAL TENSION, SYMMETRIC SHEAR VARIATION, $\mu = 0{\cdot}75$

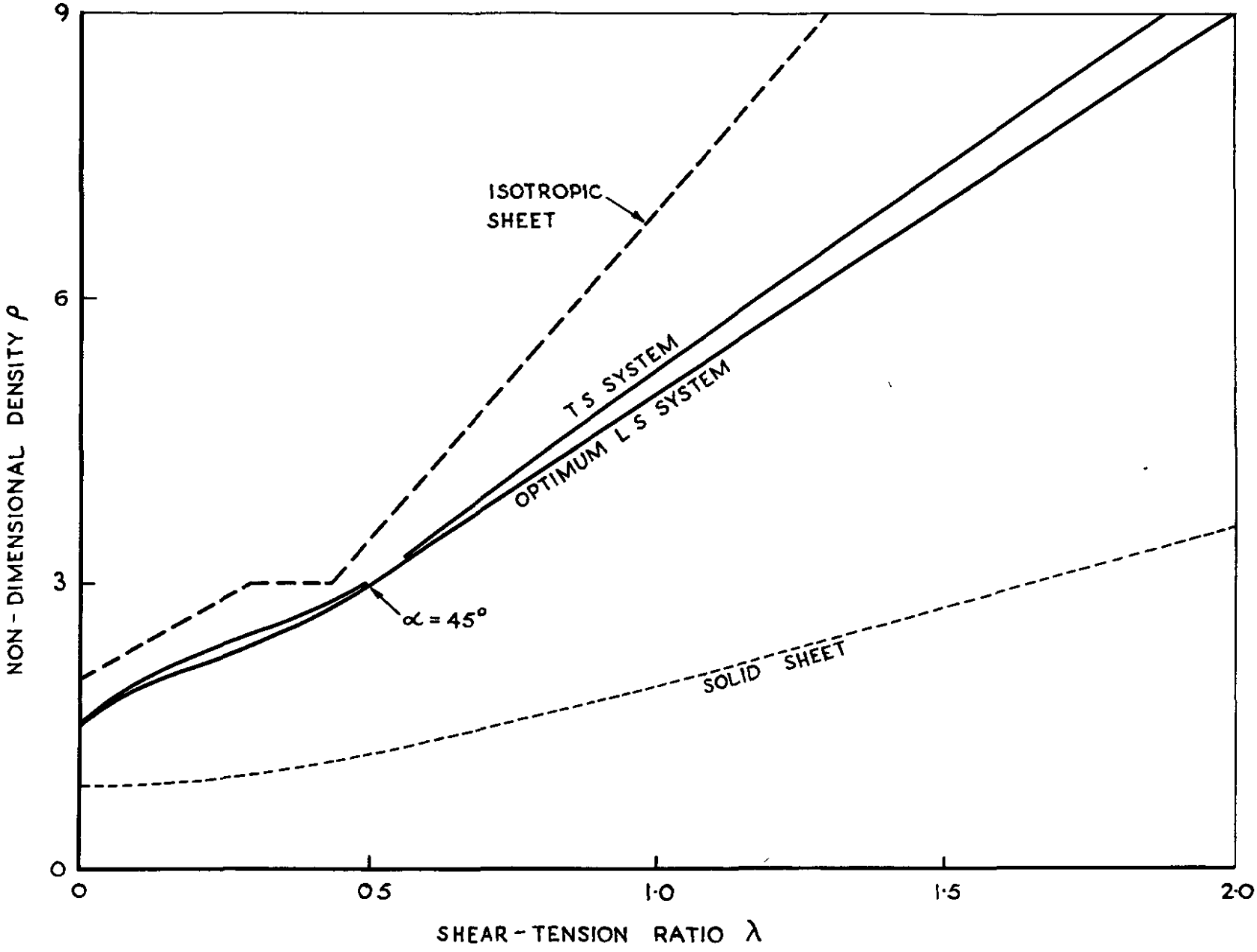

FIG.10 FIBRE DENSITIES; BIAXIAL TENSION, SYMMETRIC SHEAR VARIATION, $\mu = 0{\cdot}5$

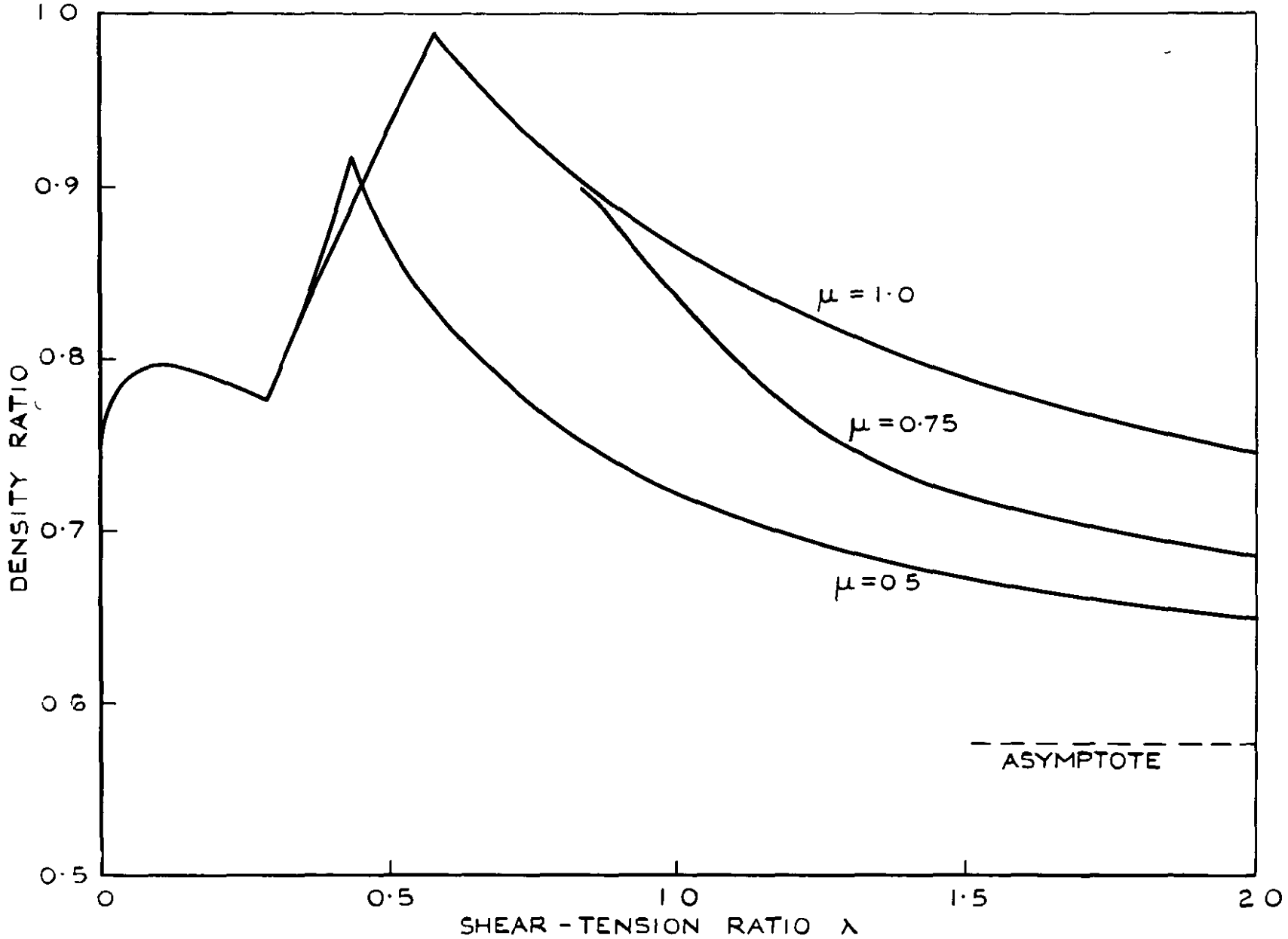

FIG 11 OPTIMUM / ISOTROPIC DENSITY RATIO ; BIAXIAL TENSION, SYMMETRIC SHEAR VARIATION

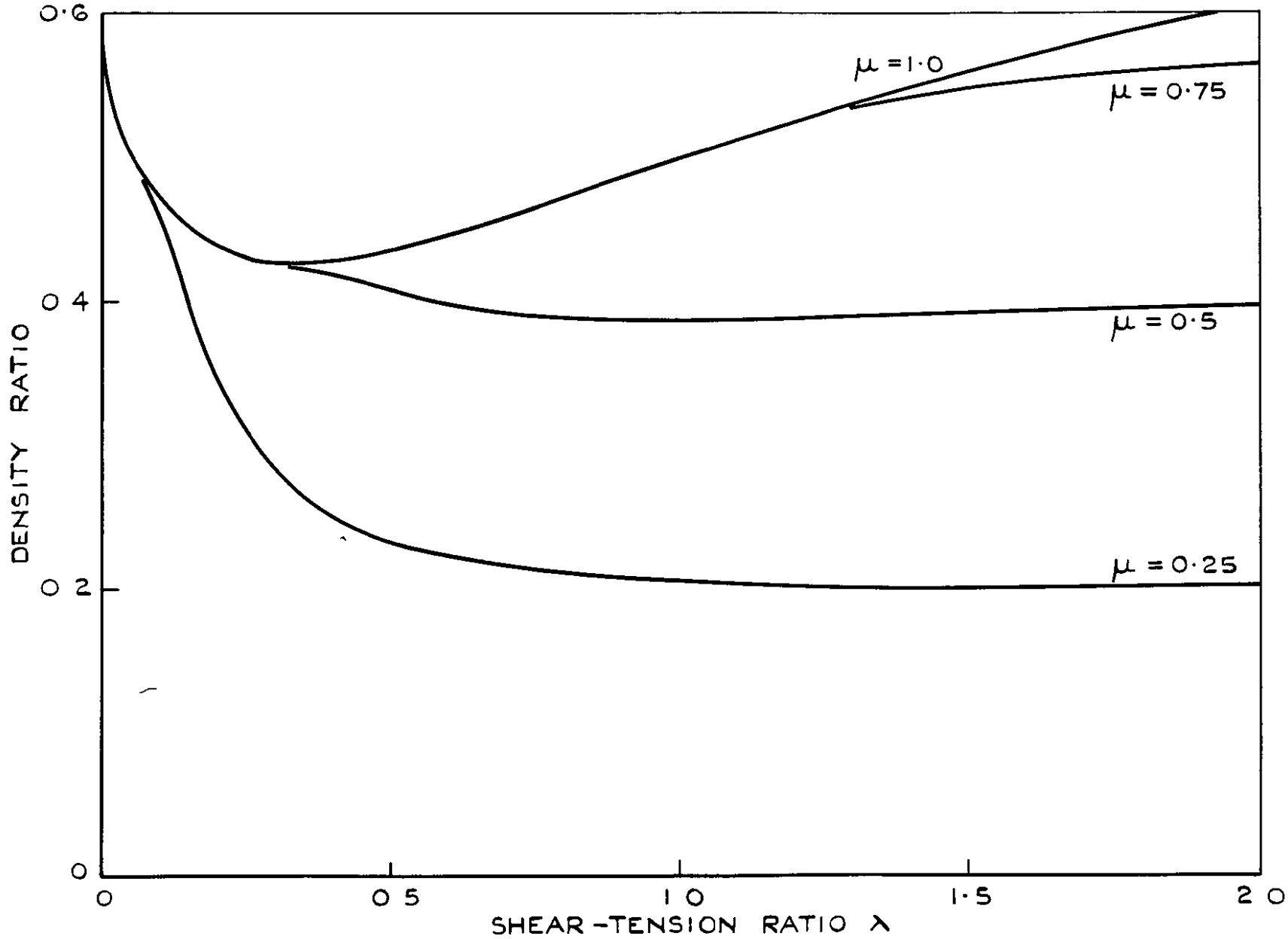

FIG.12 SOLID/OPTIMUM DENSITY RATIO; BIAXIAL TENSION, SYMMETRIC SHEAR VARIATION

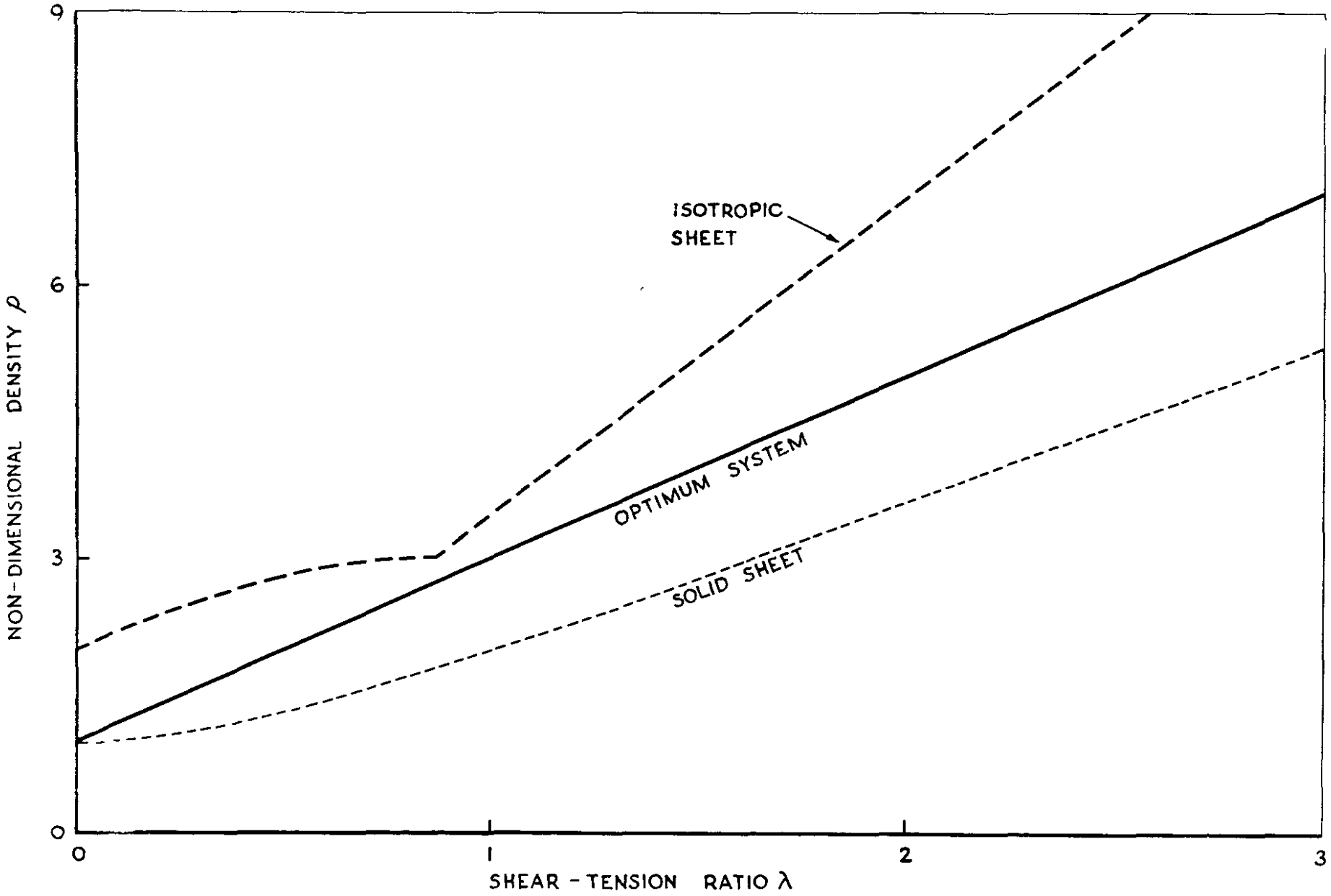

FIG. 13 FIBRE DENSITIES; UNIAXIAL TENSION, ASYMMETRIC SHEAR VARIATION, $\mu = 1$

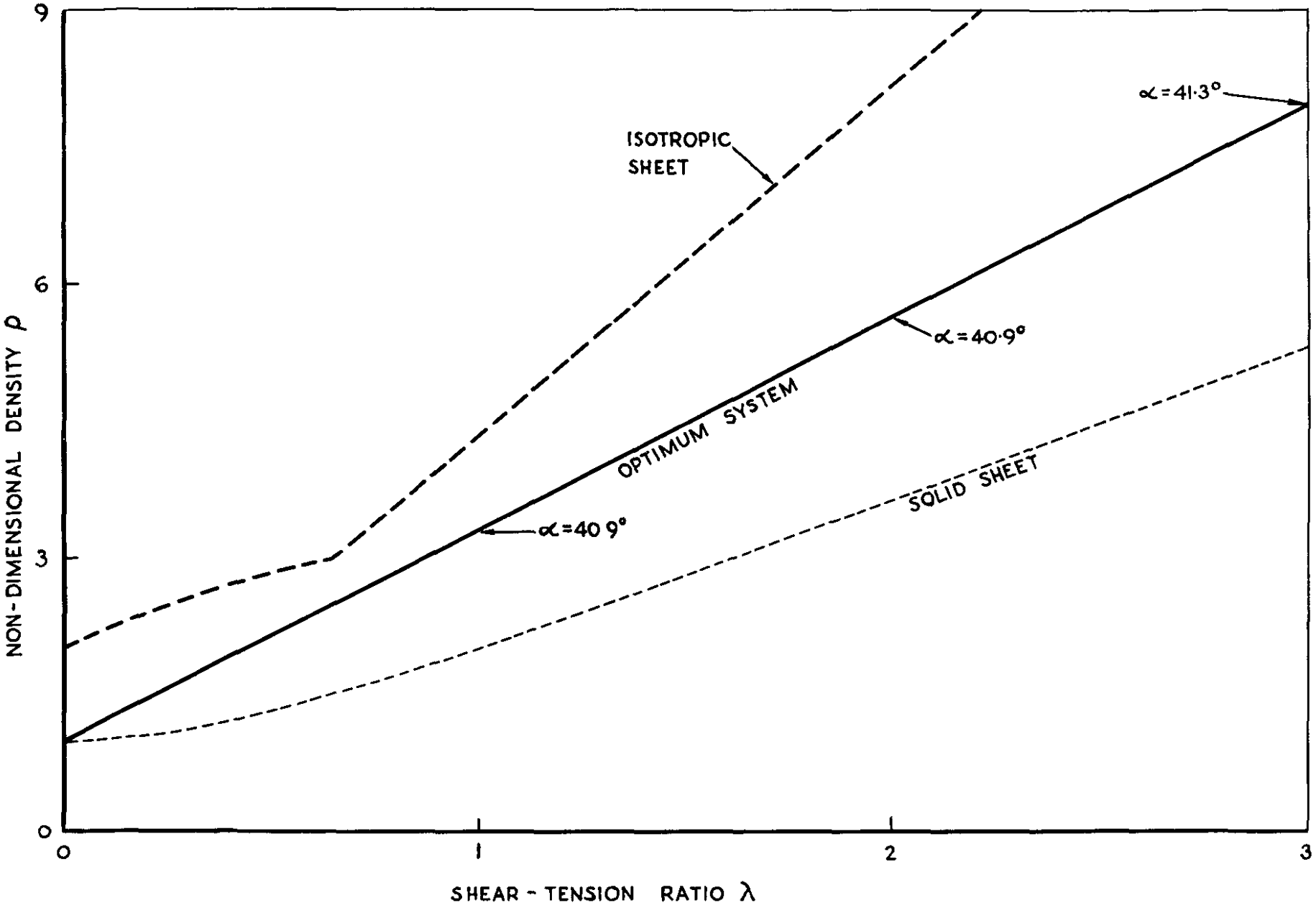

FIG. 14 FIBRE DENSITIES; UNIAXIAL TENSION, ASYMMETRIC SHEAR VARIATION, $\mu = 0 \cdot 75$

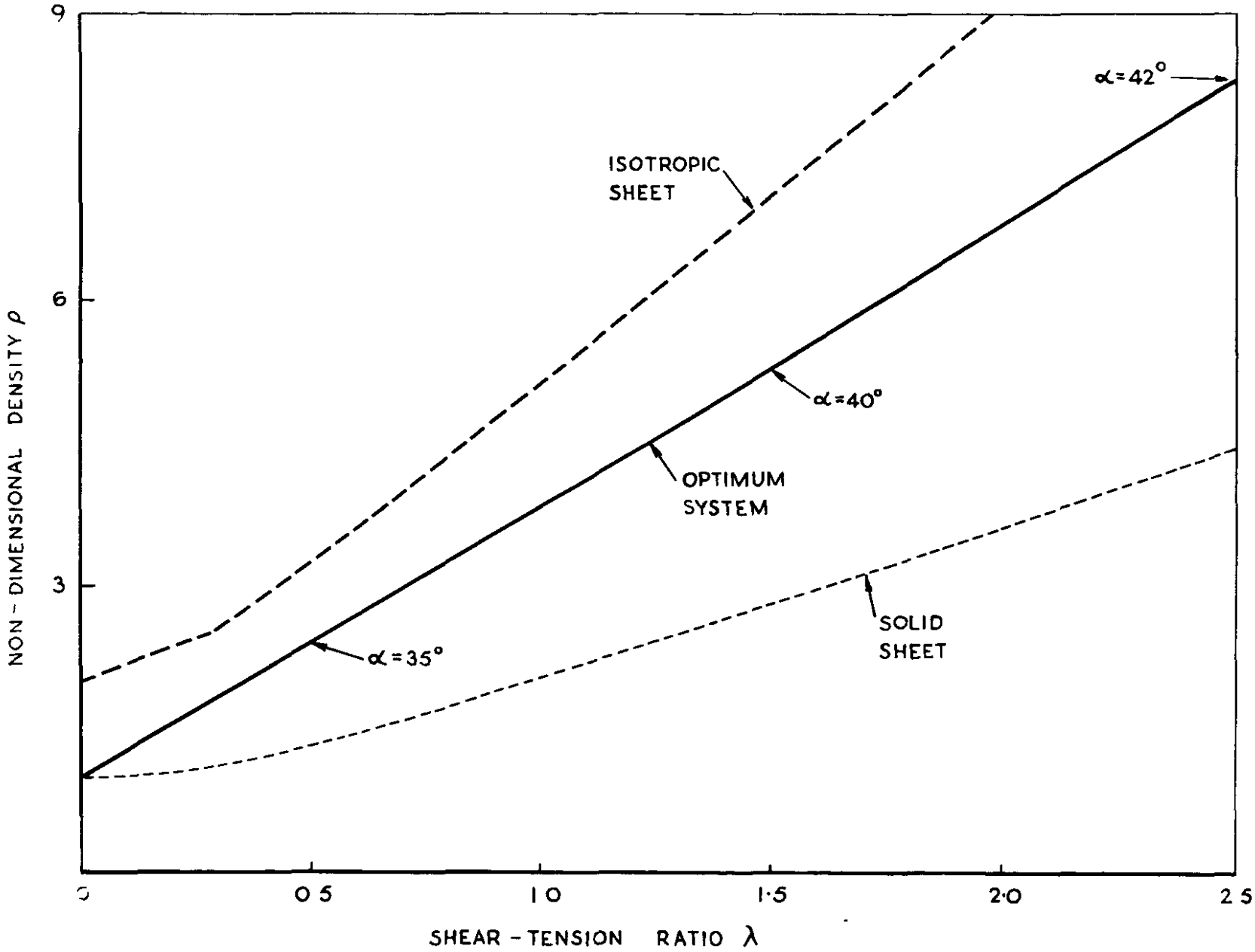

FIG. 15 FIBRE DENSITIES; UNIAXIAL TENSION, ASYMMETRIC SHEAR VARIATION, $\mu = 0{\cdot}5$

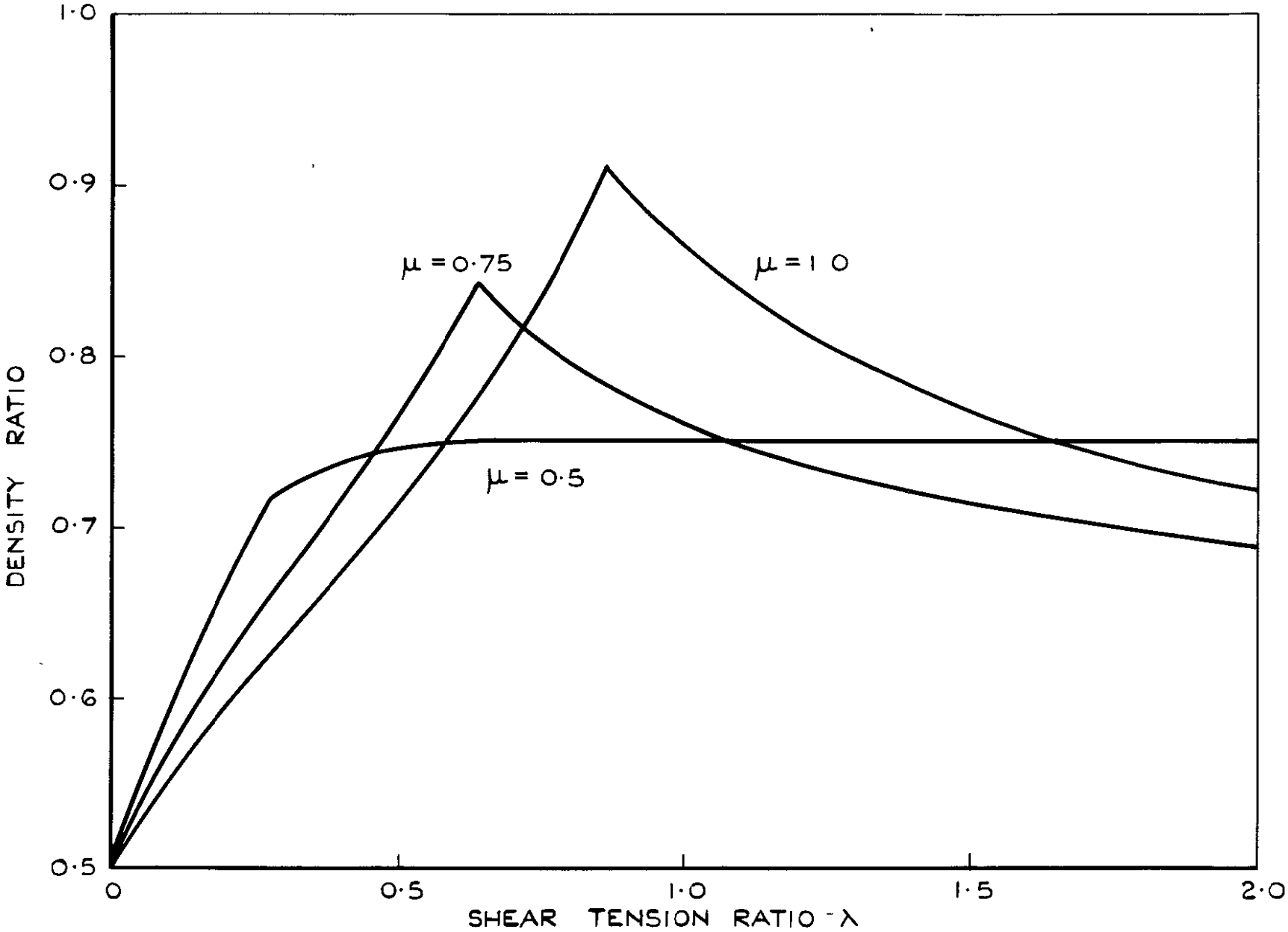

FIG. 16 OPTIMUM / ISOTROPIC DENSITY RATIO; UNIAXIAL TENSION, ASYMMETRIC SHEAR VARIATION

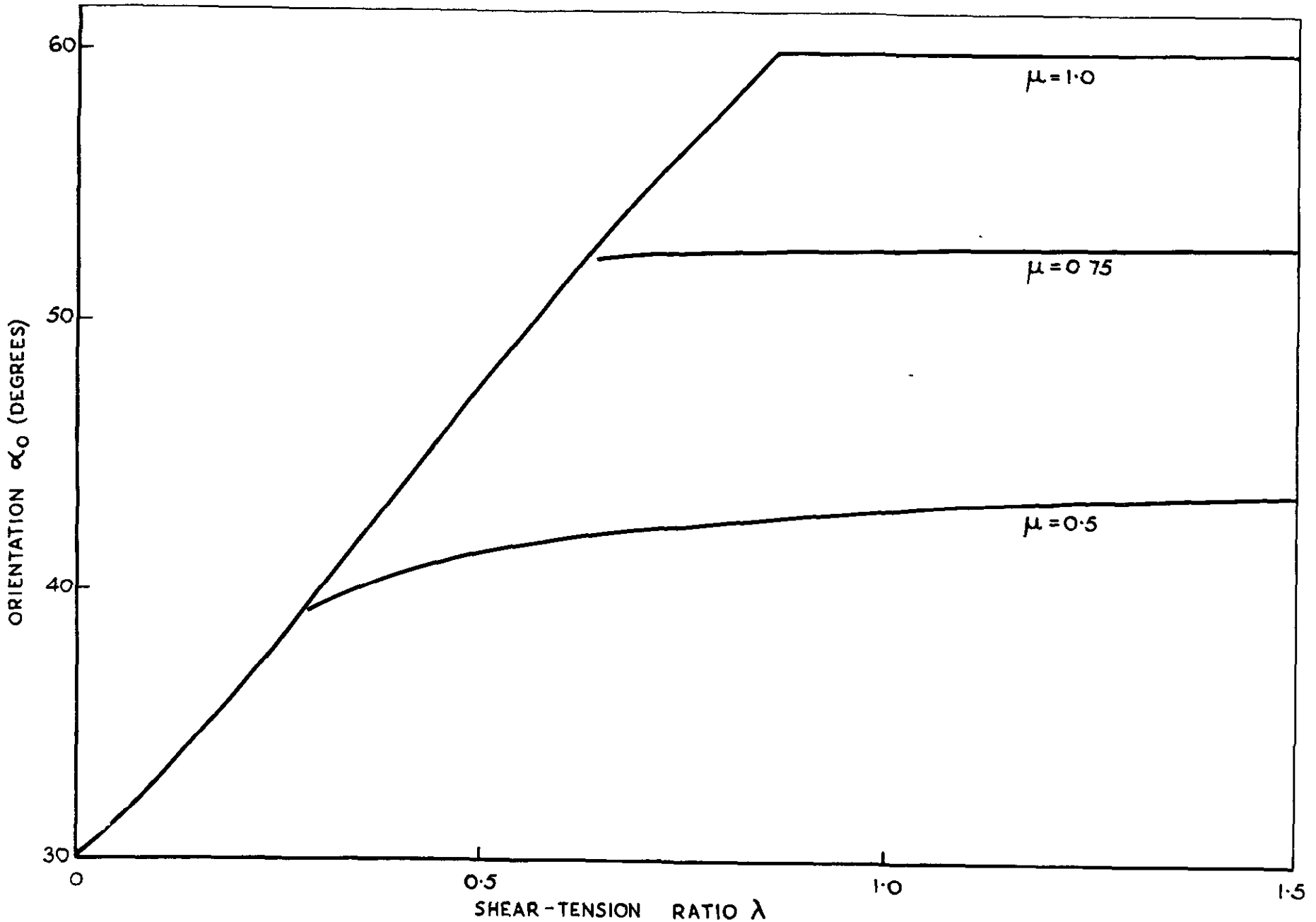

FIG. 17 ISOTROPIC ORIENTATION; UNIAXIAL TENSION, ASYMMETRIC SHEAR VARIATION

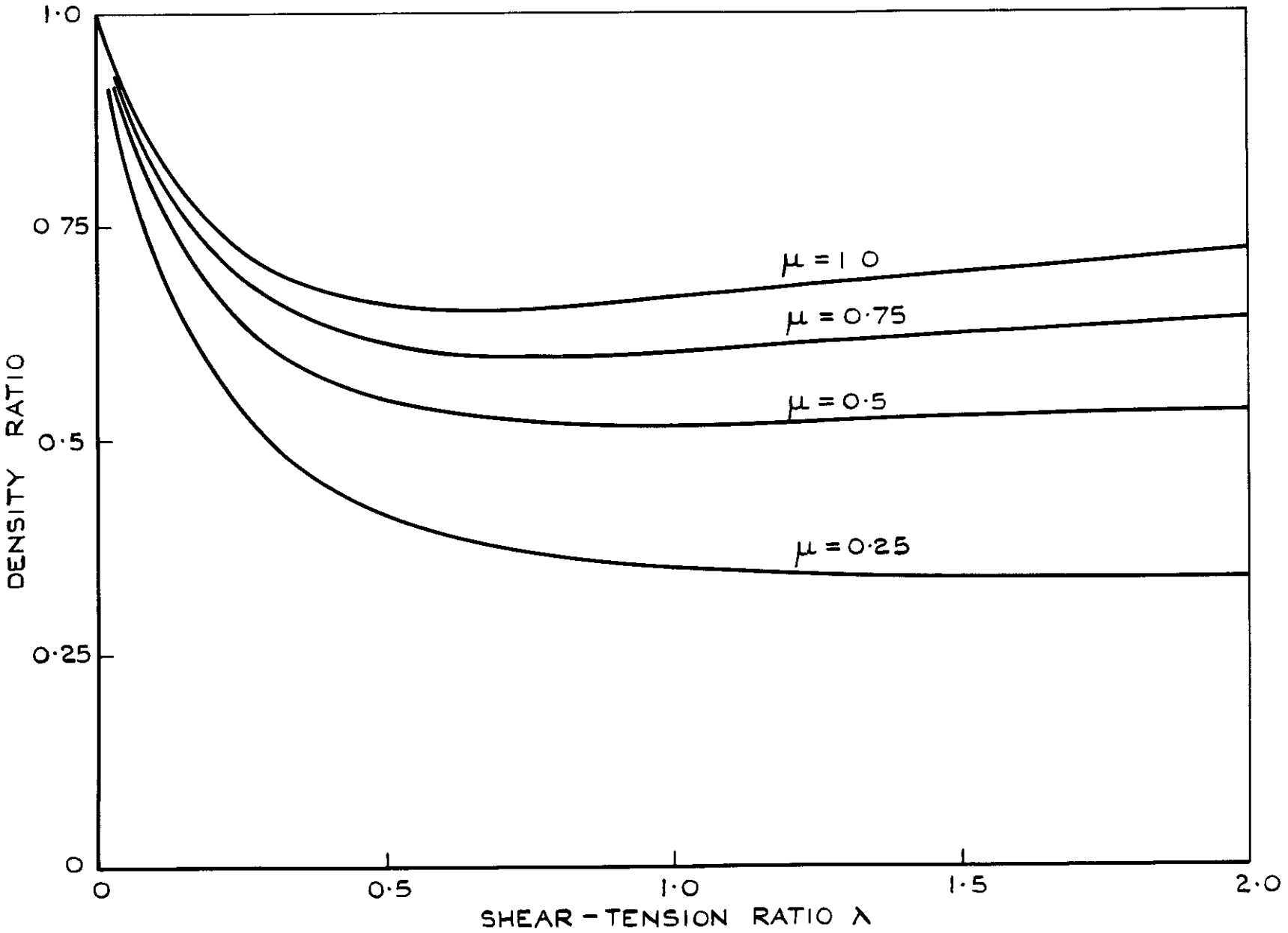

FIG. 18 SOLID / OPTIMUM DENSITY RATIO; UNIAXIAL TENSION, ASYMMETRIC SHEAR VARIATION

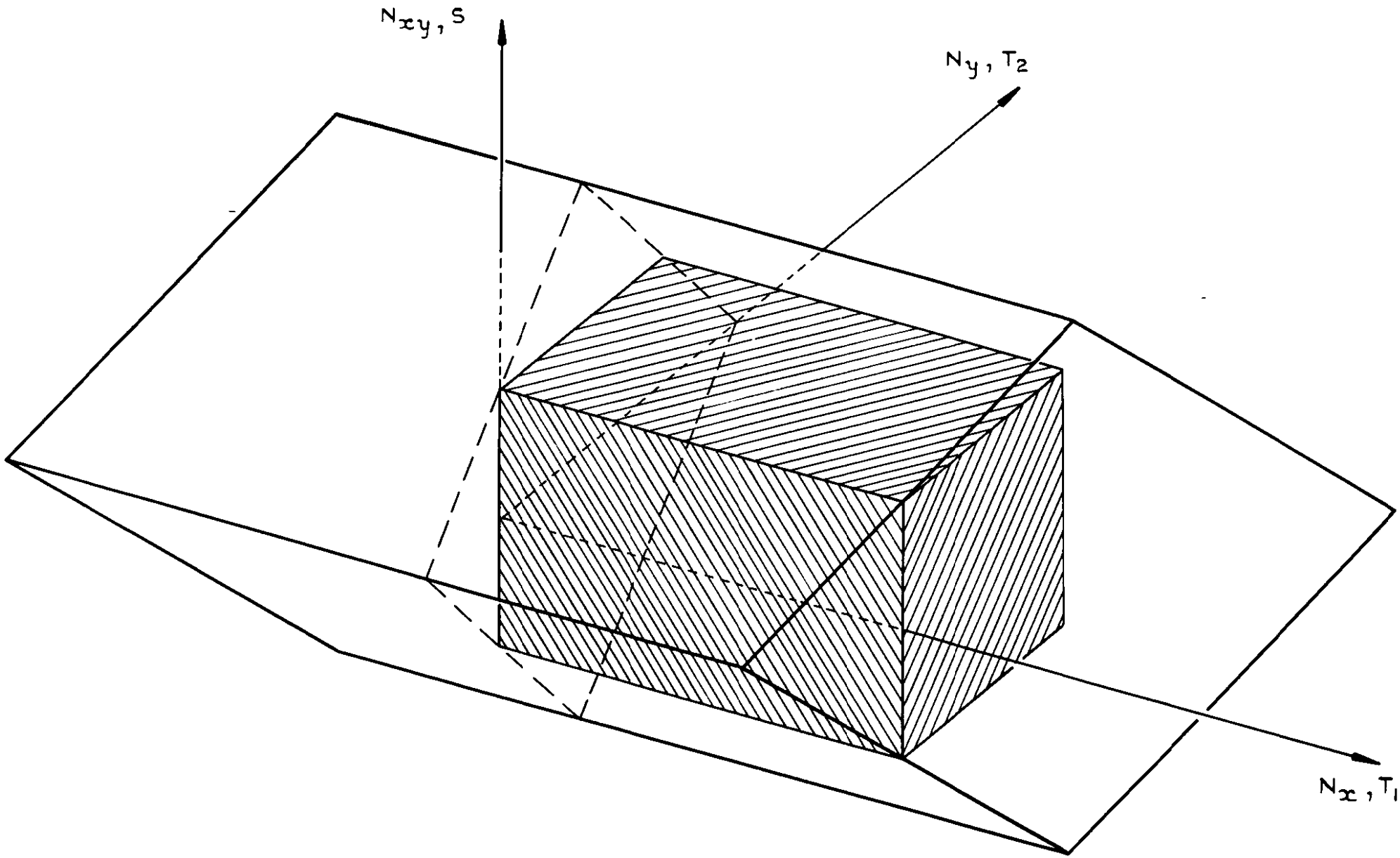

FIG.19 SCHEMATIC LOAD ENVELOPE ; LONGITUDINALLY SYMMETRIC ARRANGEMENTS

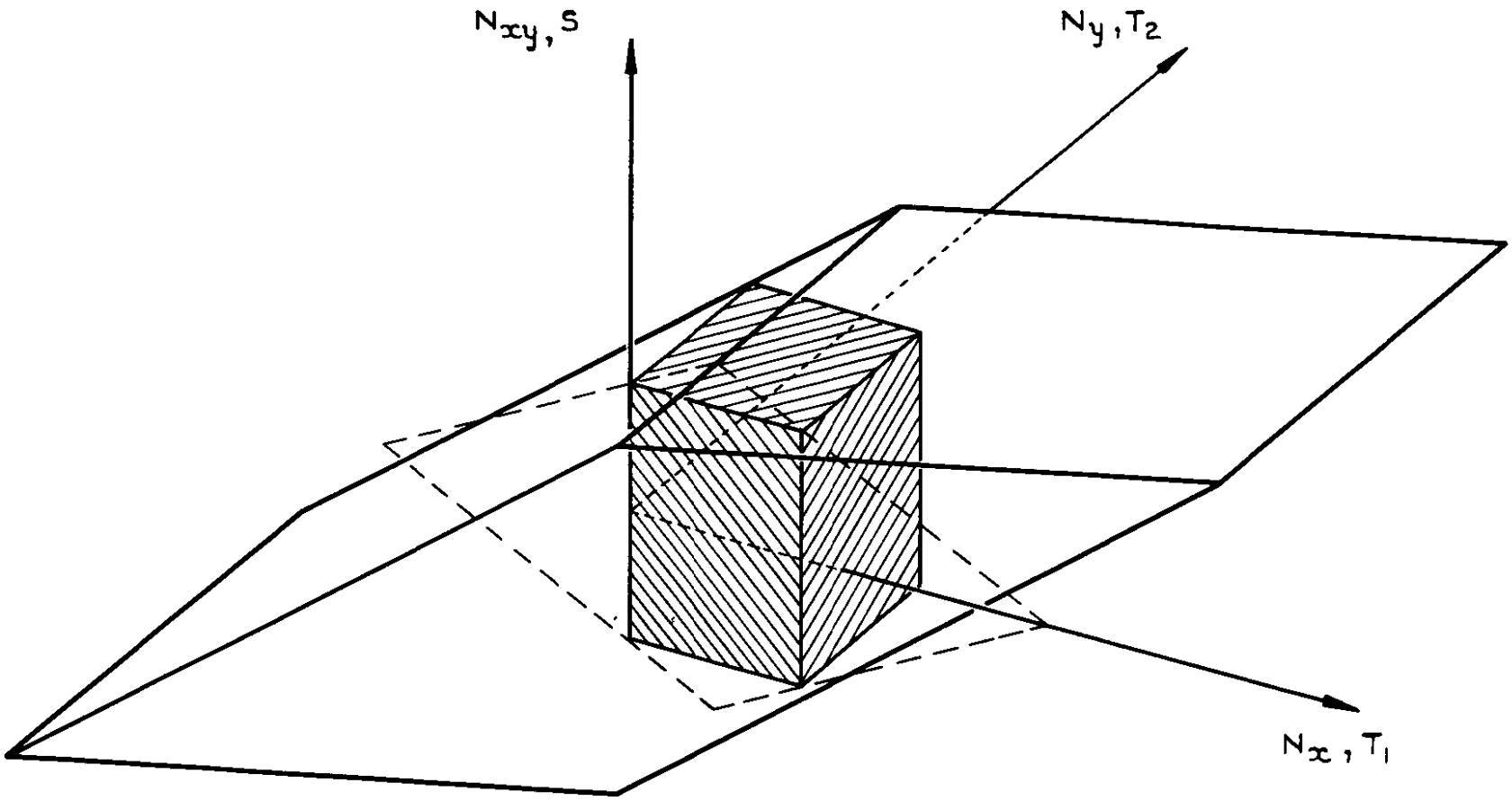

FIG 20 SCHEMATIC LOAD ENVELOPE ; TRANSVERSELY SYMMETRIC ARRANGEMENTS

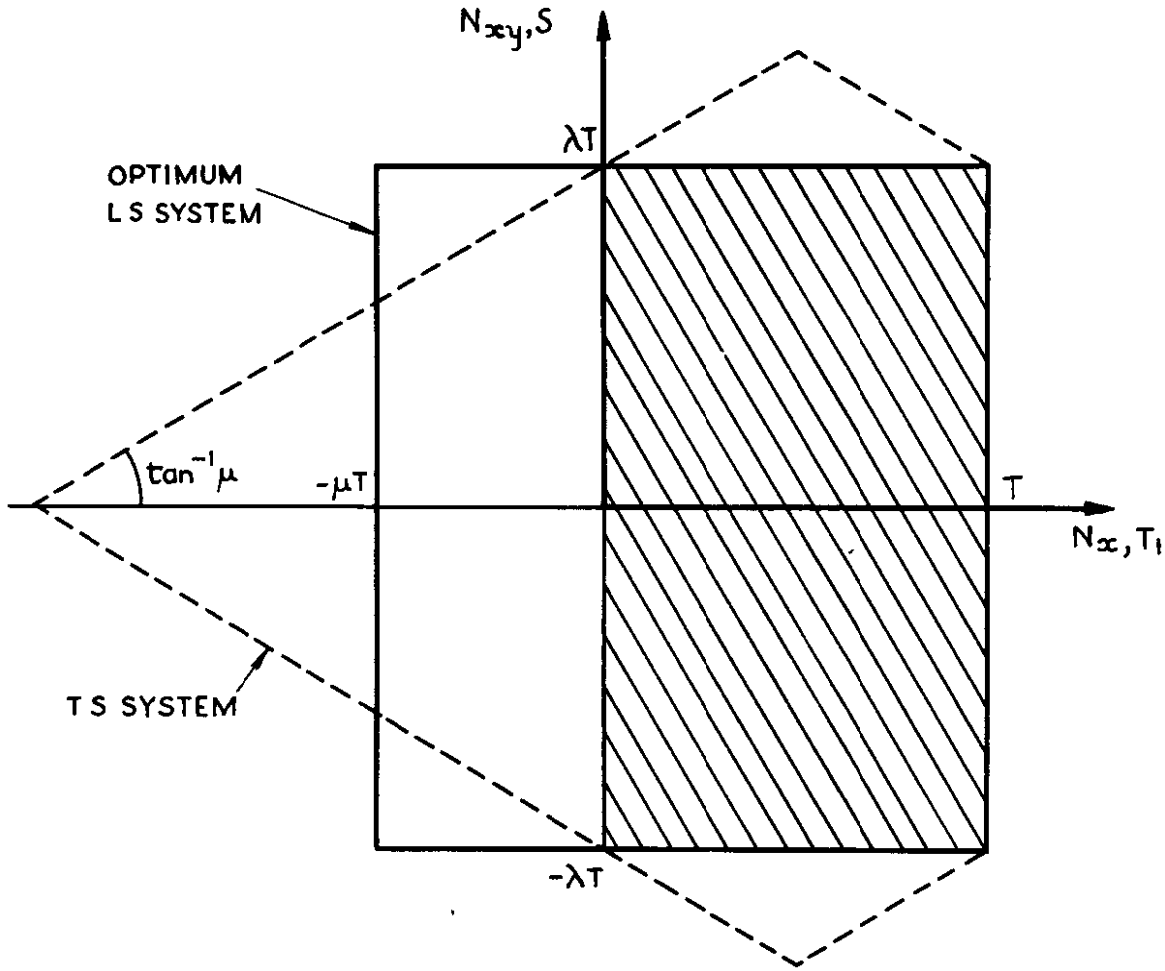

FIG 21 VARIATIONS IN PERMITTED APPLIED LOAD, SYMMETRIC ARRANGEMENTS, $\mu = 0{\cdot}6$

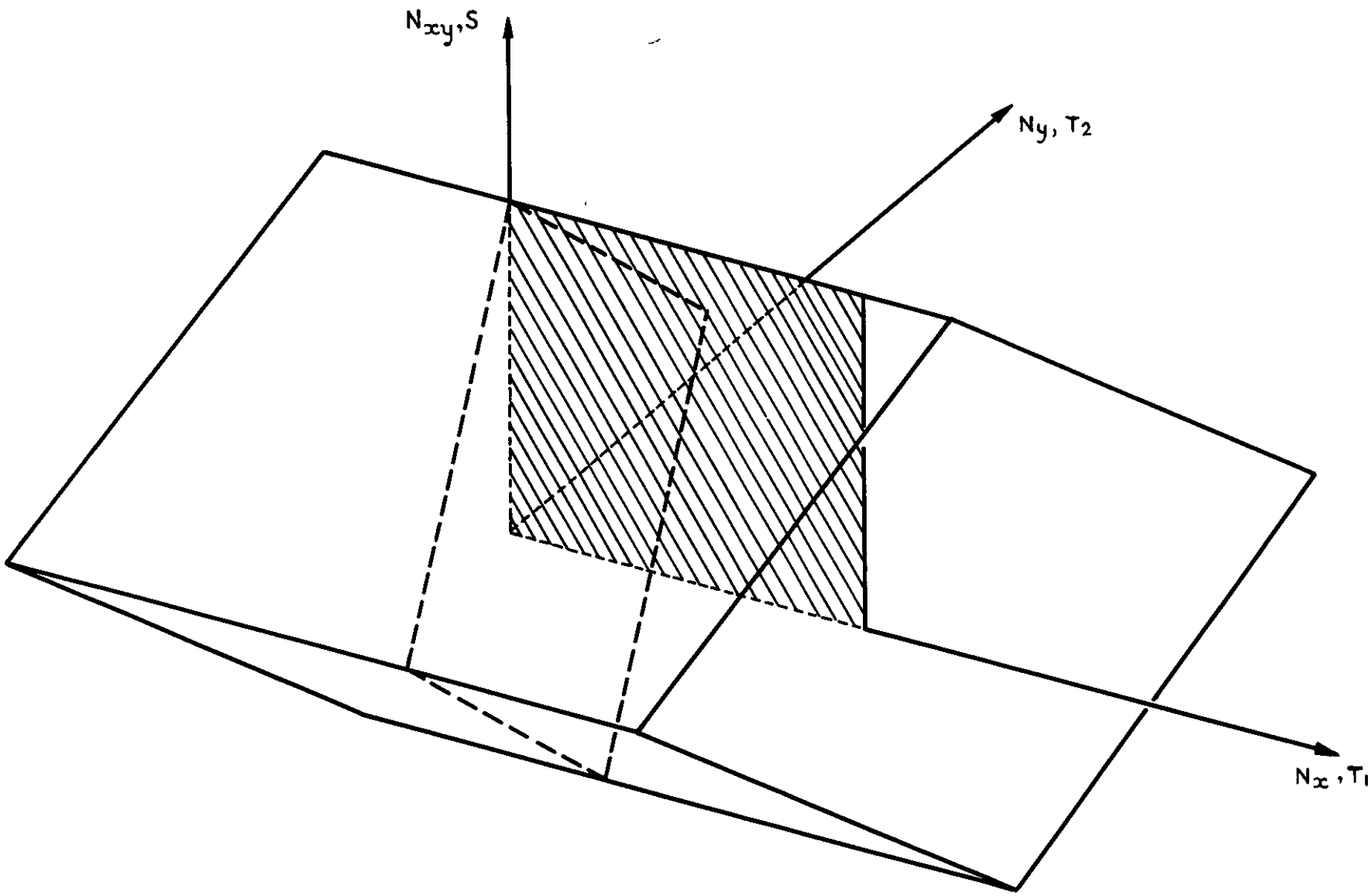

FIG. 22 SCHEMATIC LOAD ENVELOPE; ASYMMETRIC ARRANGEMENTS

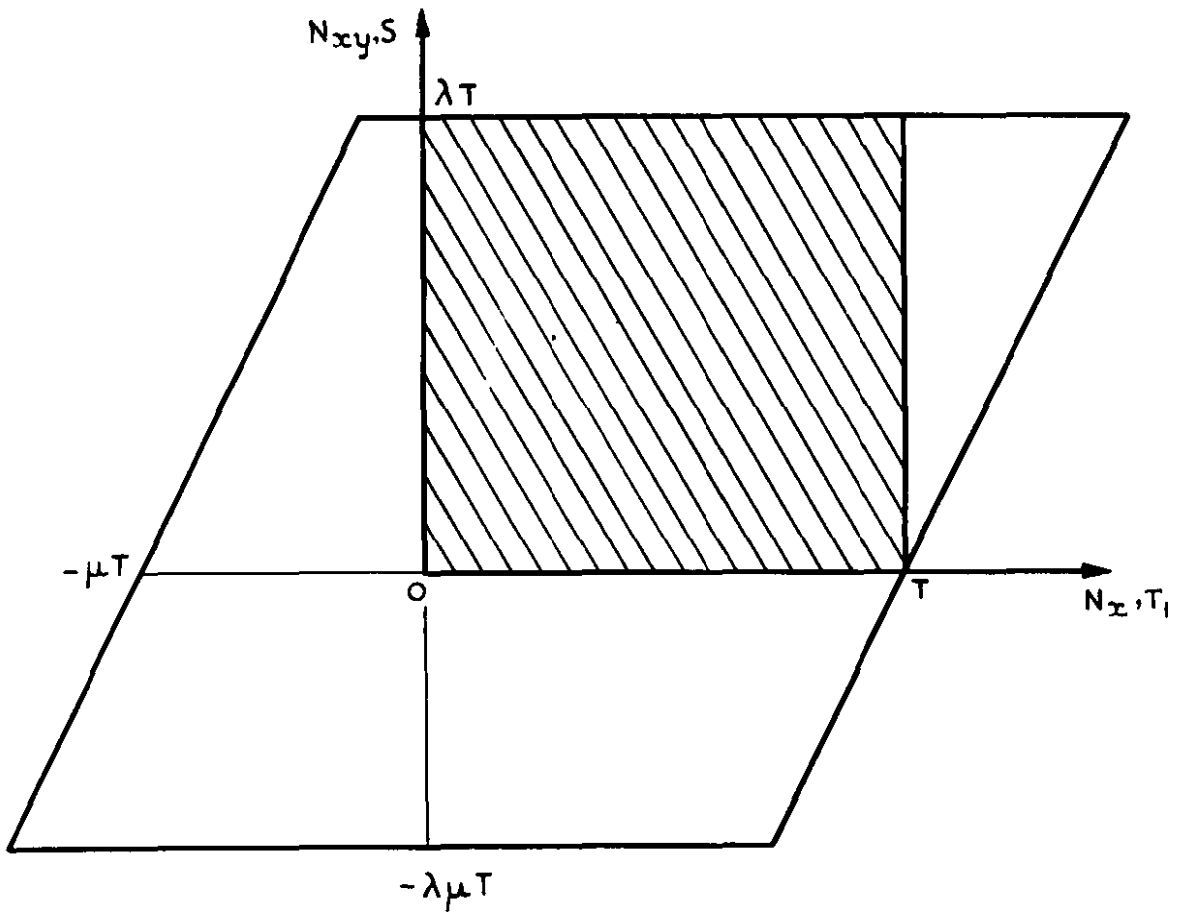

FIG. 23 VARIATION IN PERMITTED APPLIED LOAD; ASYMMETRIC ARRANGEMENT, $\mu = 0{\cdot}6$

Printed in England for Her Majesty's Stationery Office by the Royal Aircraft Establishment, Farnborough. Dd.129528. K.4.

A.R.C. C.P. No.975
November 1966

Harris, G. Z.

621-419.9 :
620.172.2 :
539.42 :
539.376

OPTIMUM FIBRE ARRANGEMENTS FOR REINFORCED SHEETS UNDER COMBINED LOADING

Sheets having three directions of fibre reinforcement are considered on the basis of netting analysis. Load envelopes of shear combined with both uniaxial and biaxial tension are assumed and optimum fibre arrangements are determined on the assumption that limits exist on the compressive and tensile forces which may be developed in a fibre. Such optimum fibre arrangements are compared with the best-arranged isotropic reinforced sheets and with hypothetical solid sheets having the same properties as the fibres. The total allowable load envelopes of the optimum arrangements are derived and are related to the prescribed load envelopes. The elastic constants of the optimum systems are also derived.

A.R.C. C.P. No.975
November 1966

Harris, G. Z.

621-419.9 :
620.172.2 :
539.42 :
539.376

OPTIMUM FIBRE ARRANGEMENTS FOR REINFORCED SHEETS UNDER COMBINED LOADING

Sheets having three directions of fibre reinforcement are considered on the basis of netting analysis. Load envelopes of shear combined with both uniaxial and biaxial tension are assumed and optimum fibre arrangements are determined on the assumption that limits exist on the compressive and tensile forces which may be developed in a fibre. Such optimum fibre arrangements are compared with the best-arranged isotropic reinforced sheets and with hypothetical solid sheets having the same properties as the fibres. The total allowable load envelopes of the optimum arrangements are derived and are related to the prescribed load envelopes. The elastic constants of the optimum systems are also derived.

A.R.C. C.P. No.975
November 1966

Harris, G. Z.

621-419.9 :
620.172.2 :
539.42 :
539.376

OPTIMUM FIBRE ARRANGEMENTS FOR REINFORCED SHEETS UNDER COMBINED LOADING

November 1966

Sheets having three directions of fibre reinforcement are considered on the basis of netting analysis. Load envelopes of shear combined with both uniaxial and biaxial tension are assumed and optimum fibre arrangements are determined on the assumption that limits exist on the compressive and tensile forces which may be developed in a fibre. Such optimum fibre arrangements are compared with the best-arranged isotropic reinforced sheets and with hypothetical solid sheets having the same properties as the fibres. The total allowable load envelopes of the optimum arrangements are derived and are related to the prescribed load envelopes. The elastic constants of the optimum systems are also derived.

DETACHABLE ABSTRACT CARDS

Published by
HER MAJESTY'S STATIONERY OFFICE

To be purchased from
49 High Holborn, London W C 1
423 Oxford Street, London W 1
13A Castle Street, Edinburgh 2
109 St. Mary Street, Cardiff
Brazennose Street, Manchester 2
50 Fairfax Street, Bristol 1
258-259 Broad Street, Birmingham 1
7-11 Linenhall Street, Belfast 2
or through any bookseller

S.O. CODE No. 23-9017-75